

Electronic Supplementary Material (ESI) for Physical Chemistry Chemical Physics.
This journal is © the Owner Societies 2023

*Electronic Supporting Information for
the manuscript*

Probing the Dynamic Behaviour and Magnetic Identification of Seven Coordinated Mn(II) Complexes: A Combined AIMD and Multi-reference Approach†

Niharika Keot^a and Manabendra Sarma^{a*}

^aDepartment of Chemistry, Indian Institute of Technology Guwahati 781039, India

*Email: msarma@iitg.ac.in

Table of Contents

List of Tables		Page No.
Table S1	RMSD value of the structures was calculated at 2 ps intervals against the Crystal structure using discovery studio and Pymol (at 25°C).	12
Table S2	RMSD value of the structures was calculated at 2 ps intervals against the Crystal structure using discovery studio and Pymol (90°C).	12-13
Table S3	Bond length and bond angles of the Mn(II) complexes (temperature annealing+geometry optimization) with their crystallographic structure.	13-14
Table S4	Binding energy values and relative binding energy (ΔE_{REL}) values (in kcal mol ⁻¹) of the chosen complexes at 25°C.	15
Table S5	Spin–Orbit Coupling (SOC) and Spin–Spin (SS) Contributions to the D Values (cm ⁻¹) Calculated using TPSS/def2-TZVP level of theory.	16
Table S6	Spin–Orbit Coupling (SOC) and Spin–Spin (SS) Contributions to the D Values (cm ⁻¹) Calculated using M06-2X/def2-TZVP level of theory.	16-17
Table S7	ZFS parameter of all the complexes using M06-2X/def2-TZVP.	17-18
Table S8	NEVPT2 transition energy and their individual contribution to the D values for Complex 1 (up to 17 quartets and 13 doublets are shown).	18-19
Table S9	NEVPT2 transition energy and their individual contribution to the D values for Complex 2 (up to 17 quartets and 13 doublets are shown).	19-20
Table S10	NEVPT2 transition energy and their individual contribution to the D values for Complex 3 (up to 17 quartets and 13 doublets are shown).	20-21
Table S11	NEVPT2 transition energy and their individual contribution to the D values for Complex 4 (up to 17 quartets and 13 doublets are shown).	22-23

Table S12	NEVPT2 transition energy and their individual contribution to the D values for Complex 5 (up to 17 quartets and 13 doublets are shown).	23
Table S13	NEVPT2 transition energy and their individual contribution to the D values for Complex 6 (up to 17 quartets and 13 doublets are shown).	24
Table S14	NEVPT2 transition energy and their individual contribution to the D values for Complex 7 (up to 17 quartets and 13 doublets are shown).	25
Table S15	NEVPT2 transition energy and their individual contribution to the D values for Complex 8 (up to 17 quartets and 13 doublets are shown).	26
Table S16	NEVPT2 transition energy and their individual contribution to the D values for Complex 9 (up to 17 quartets and 13 doublets are shown).	27
Table S17	NEVPT2 transition energy and their individual contribution to the D values for Complex 10 (up to 17 quartets and 13 doublets are shown).	28
Table S18	NEVPT2 transition energy and their individual contribution to the D values for Complex 11 (up to 17 quartets and 13 doublets are shown).	29
Table S19	NEVPT2 transition energy and their individual contribution to the D values for Complex 12 (up to 17 quartets and 13 doublets are shown).	30
Table S20	NEVPT2 transition energy and their individual contribution to the D values for Complex 13 (up to 17 quartets and 13 doublets are shown).	31
Table S21	NEVPT2 transition energy and their individual contribution to the D values for Complex 14 (up to 17 quartets and 13 doublets are shown).	32
Table S22	NEVPT2 transition energy and their individual contribution to the D values for Complex 15 (up to 17 quartets and 13 doublets are shown).	33
Table S23	NEVPT2 transition energy and their individual contribution to the D values for Complex 16 (up to 17 quartets and 13 doublets are shown).	34
Table S24	NEVPT2 transition energy and their individual contribution to the D values for Complex 17 (up to 17 quartets and 13 doublets are shown).	35
Table S25	NEVPT2 transition energy and their individual contribution to the D values for Complex 18 (up to 17 quartets and 13 doublets are shown).	36
Table S26	NEVPT2 transition energy and their individual contribution to the D values for Complex 19 (up to 17 quartets and 13 doublets are shown).	37
Table S27	NEVPT2 transition energy and their individual contribution to the D values for Complex 20 (up to 17 quartets and 13 doublets are shown).	38

Table S28	Racah-parameters and spin-orbit coupling parameters for free Metal ion (Mn^{2+}) and complexes AILFT parameters (in cm^{-1}) from AILFT calculations.	41-42
Table S29	Topological parameters of the complexes analyzed here; the electron density at bond critical points (ρ_{bcp}), its Laplacian ($\nabla^2 \rho_{bcp}$), and the kinetic electron energy density (G_{bcp}). The results obtained at M06-2X/def2-TZVP level of approximation correspond to Mn-O, Mn-S, and Mn-Se bonds.	42-43
Table S30	NPA charge analysis obtained at the M06-2X/def2-TZVP level of theory.	43
Table S31	Mayer bond order obtained at the M06-2X/def2-TZVP level of theory.	43
Table S32	Atomic Cartesian coordinates (\AA) of the PBE/GTH-DZVP optimized structure of the $[Mn(dpasam)(H_2O)]^-$ complex. Only the water molecules directly coordinated with the Mn^{2+} ion are included.	44-45
Table S33	Atomic Cartesian coordinates (\AA) of the PBE/GTH-DZVP optimized structure of the $[Mn(dpaaa)(H_2O)]^-$ complex. Only the water molecules directly coordinated with the Mn^{2+} ion are included.	46-47
Table S34	Atomic Cartesian coordinates (\AA) of the PBE/GTH-DZVP optimized structure of the $[Mn(cbda)(H_2O)]^-$ complex. Only the water molecules directly coordinated with the Mn^{2+} ion are included.	47-48
Table S35	Atomic Cartesian coordinates (\AA) of the PBE/GTH-DZVP optimized structure of the $[Mn(pydpa)(H_2O)]$ complex. Only the water molecules directly coordinated with the Mn^{2+} ion are included.	49-50

List of Figures

Figure S1	Potential energy (Hartree) plots at 25°C for AIMD trajectories of simulated complexes. a) $[Mn(dpasam)(H_2O)]^-$, b) $[Mn(dpaaa)(H_2O)]^-$, c) $[Mn(cbda)(H_2O)]^-$, d) $[Mn(pydpa)(H_2O)]$ complex. Orange lines indicate the equilibrated portions of AIMD trajectories used to get the radial distribution functions and further study.	5
Figure S2	Potential energy (Hartree) plots at 90°C for AIMD trajectories of simulated complexes. a) $[Mn(dpasam)(H_2O)]^-$, b) $[Mn(dpaaa)(H_2O)]^-$, c) $[Mn(cbda)(H_2O)]^-$, d) $[Mn(pydpa)(H_2O)]$ complex.	6
Figure S3	Radial distribution functions (RDF) and coordination numbers (CN) of the $[Mn(dpasam)(H_2O)]^-$ (1 st row), $[Mn(dpaaa)(H_2O)]^-$ (2 nd row), $[Mn(cbda)(H_2O)]^-$ (3 rd row), and $[Mn(pydpa)(H_2O)]$ (4 th row) complex from the equilibrated AIMD trajectory for (a) Mn-C, (b) Mn-N, and (c) Mn-O bond pair at 25°C .	7
Figure S4	Plots of Mn-O bond distances, at 25°C during the AIMD trajectories of a) $[Mn(dpasam)(H_2O)]^-$ complex, b) $[Mn(dpaaa)(H_2O)]^-$ complex, c) $[Mn(cbda)(H_2O)]^-$ complex, d) $[Mn(pydpa)(H_2O)]$. Orange, blue, yellow, and grey curves represent the Mn-O distances for individual oxygen atoms along the AIMD trajectory.	8

Figure S5	Plots of Mn-N bond distances, at 25 ⁰ C during the AIMD trajectories of a) [Mn(dpasam)(H ₂ O)] ⁻ complex, b) [Mn(dpaaa)(H ₂ O)] ⁻ complex, c)[Mn(cbda)(H ₂ O)] ⁻ complex, d) [Mn(pydpa)(H ₂ O)] ⁻ . Orange, blue, yellow, and grey curves represent the Mn-O distances for individual oxygen atoms along the AIMD trajectory.	9
Figure S6	Plots of Mn-O bond distances, at 90 ⁰ C during the AIMD trajectories of a) [Mn(dpasam)(H ₂ O)] ⁻ complex, b) [Mn(dpaaa)(H ₂ O)] ⁻ complex, c)[Mn(cbda)(H ₂ O)] ⁻ complex, d) [Mn(pydpa)(H ₂ O)] ⁻ . Orange, blue, yellow, and grey curves represent the Mn-O distances for individual oxygen atoms along the AIMD trajectory.	10
Figure S7	Plots of Mn-N bond distances, at 90 ⁰ C during the AIMD trajectories of a) [Mn(dpasam)(H ₂ O)] ⁻ complex, b) [Mn(dpaaa)(H ₂ O)] ⁻ complex, c)[Mn(cbda)(H ₂ O)] ⁻ complex, d) [Mn(pydpa)(H ₂ O)]. Orange, blue, yellow, and grey curves represent the Mn-O distances for individual oxygen atoms along the AIMD trajectory.	11
Figure S8	The Optimized structure of all four complexes using PBE/DZVP with GTH pseudopotential a) [Mn(dpasam)(H ₂ O)] ⁻ , b) [Mn(dpaaa)(H ₂ O)] ⁻ , c) [Mn(cbda)(H ₂ O)] ⁻ , and d) [Mn(pydpa)(H ₂ O)]. Only the water molecule directly connected to the metal center is shown.	14
Figure S9	Variation of D values of Class II (a, b) and Class III (c, d) complexes with the energy difference between the ground and first excited $\Delta E_{(1st-GS)}$. The solid line serves only as a guide for the eye.	15
Figure S10	Splitting of metal d-orbitals obtained with AILFT calculations (a) Complex 5, (b) Complex 6, (c) Complex 7, and (d) Complex 8, respectively.	39
Figure S11	Splitting of metal d-orbitals obtained with AILFT calculations (a) Complex 9, (b) Complex 10, (c) Complex 11, and (d) Complex 12, respectively.	40

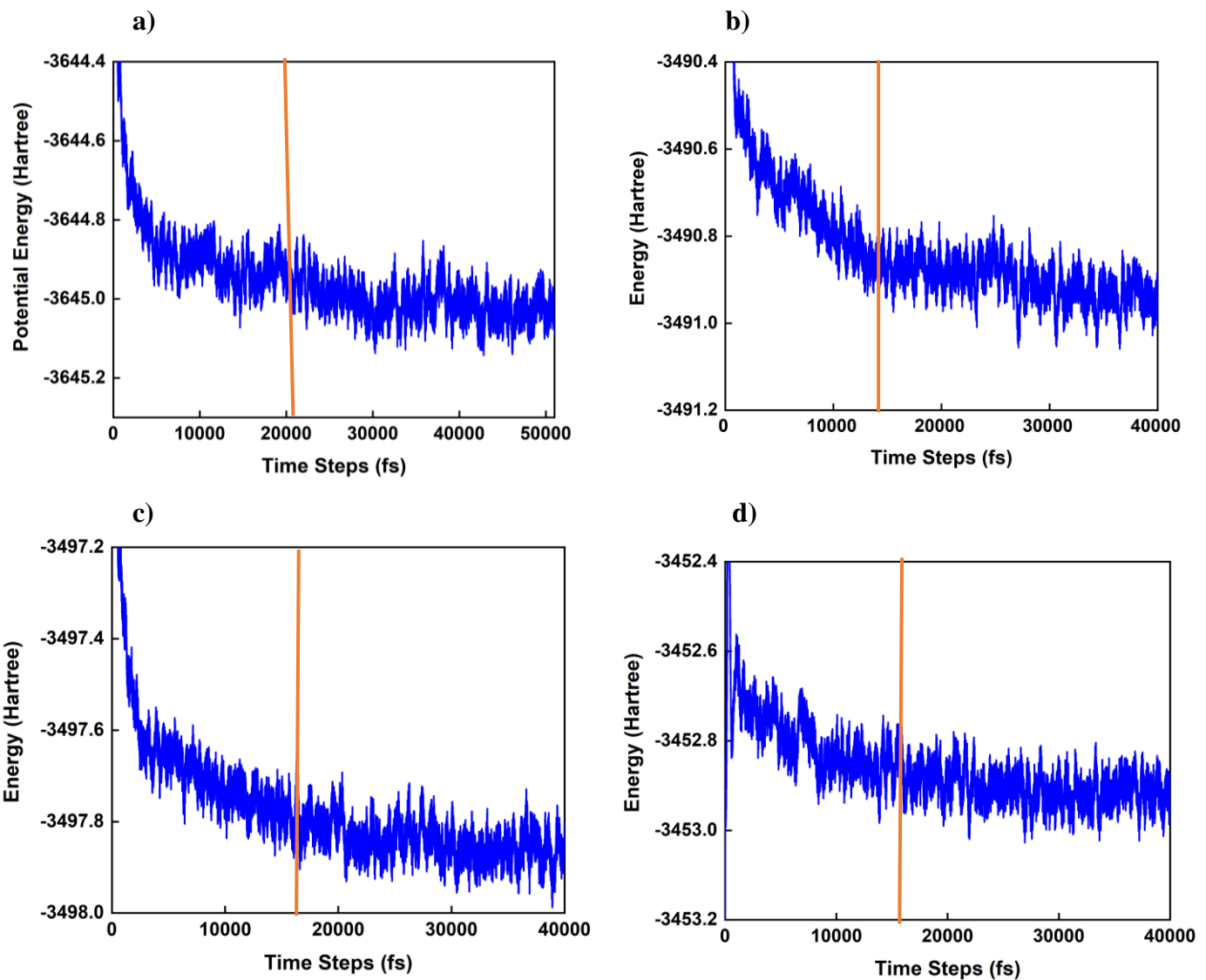


Figure S1: Potential energy (Hartree) plots at 25°C for AIMD trajectories of simulated complexes. a) [Mn(dpasam)(H₂O)]⁻, b) [Mn(dpaaa)(H₂O)]⁻, c) [Mn(cbda)(H₂O)]⁻, d) [Mn(pydpa)(H₂O)] complex. Orange lines indicate the equilibrated portions of AIMD trajectories used to get the radial distribution functions and further study.

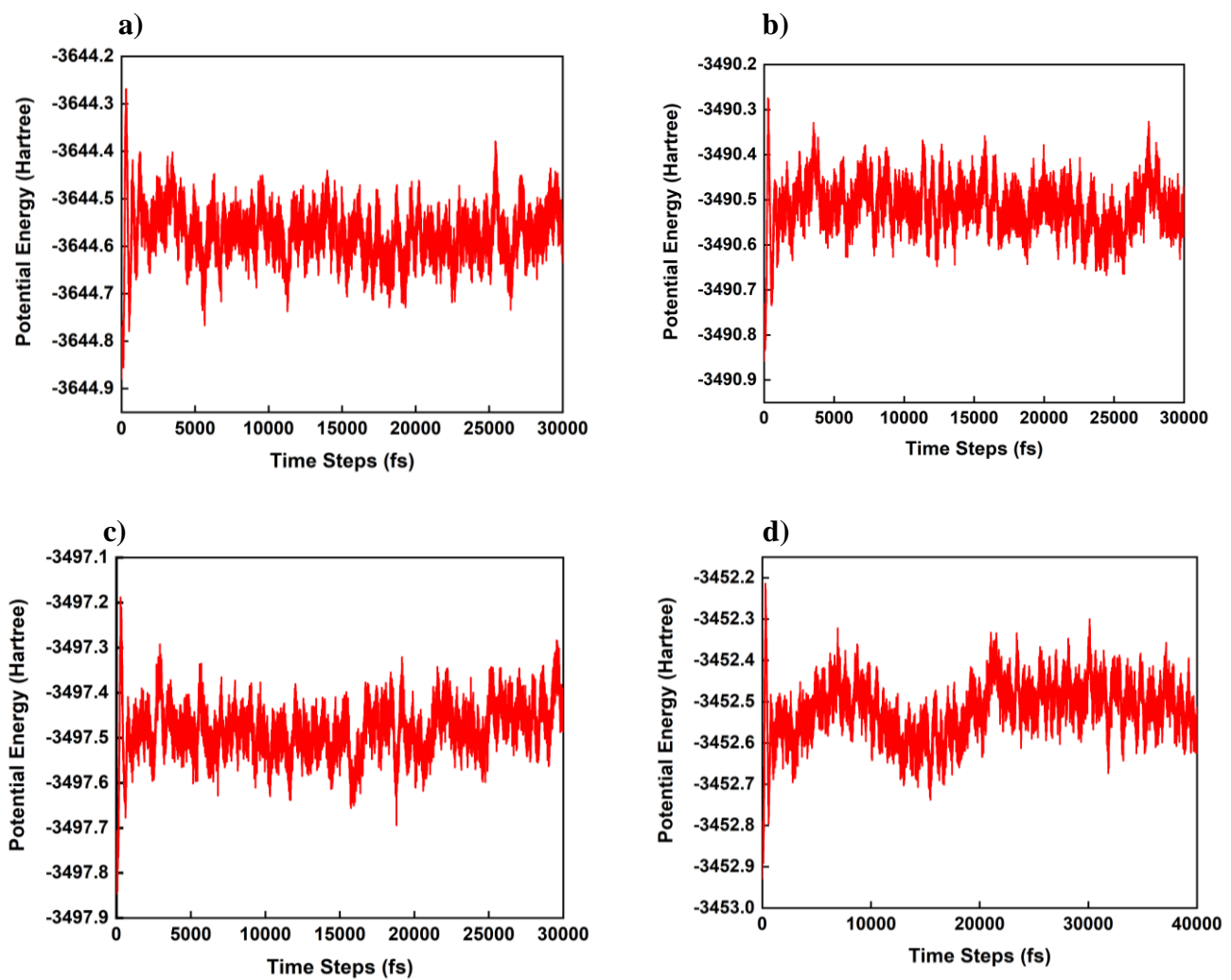


Figure S2: Potential energy (Hartree) plots at 90°C for AIMD trajectories of simulated complexes. a) $[\text{Mn}(\text{dpasam})(\text{H}_2\text{O})]^-$, b) $[\text{Mn}(\text{dpaaa})(\text{H}_2\text{O})]^-$, c) $[\text{Mn}(\text{cbda})(\text{H}_2\text{O})]^-$, d) $[\text{Mn}(\text{pydpa})(\text{H}_2\text{O})]$ complex.

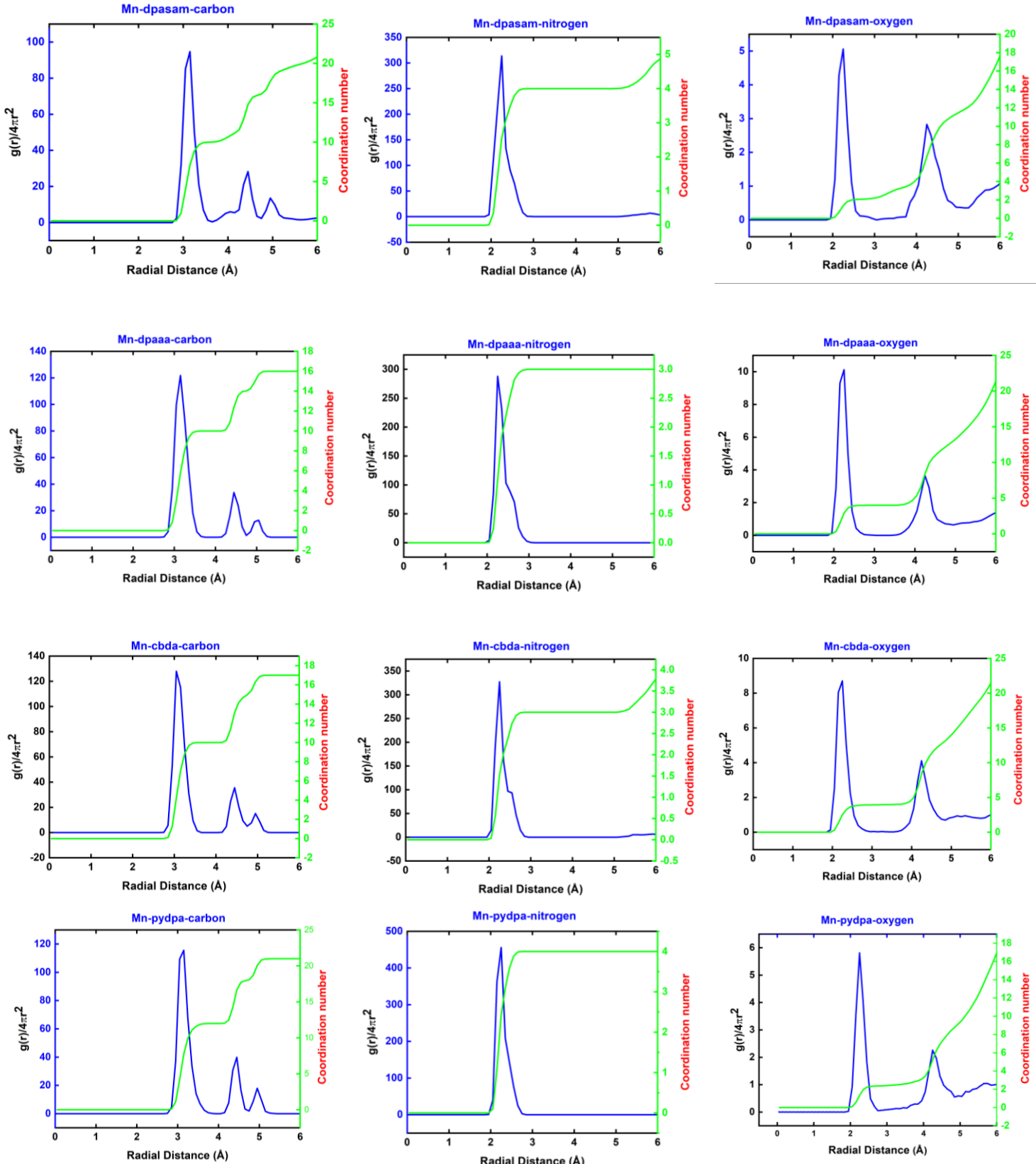


Figure S3: Radial distribution functions (RDF) and coordination numbers (CN) of the $[\text{Mn}(\text{dpasam})(\text{H}_2\text{O})]^-$ (1st row), $[\text{Mn}(\text{dpaaa})(\text{H}_2\text{O})]^-$ (2nd row), $[\text{Mn}(\text{cbda})(\text{H}_2\text{O})]^-$ (3rd row), and $[\text{Mn}(\text{pydpa})(\text{H}_2\text{O})]^-$ (4th row) complex from the equilibrated AIMD trajectory for (a) Mn–C, (b) Mn–N, and (c) Mn–O bond pair at 25°C.

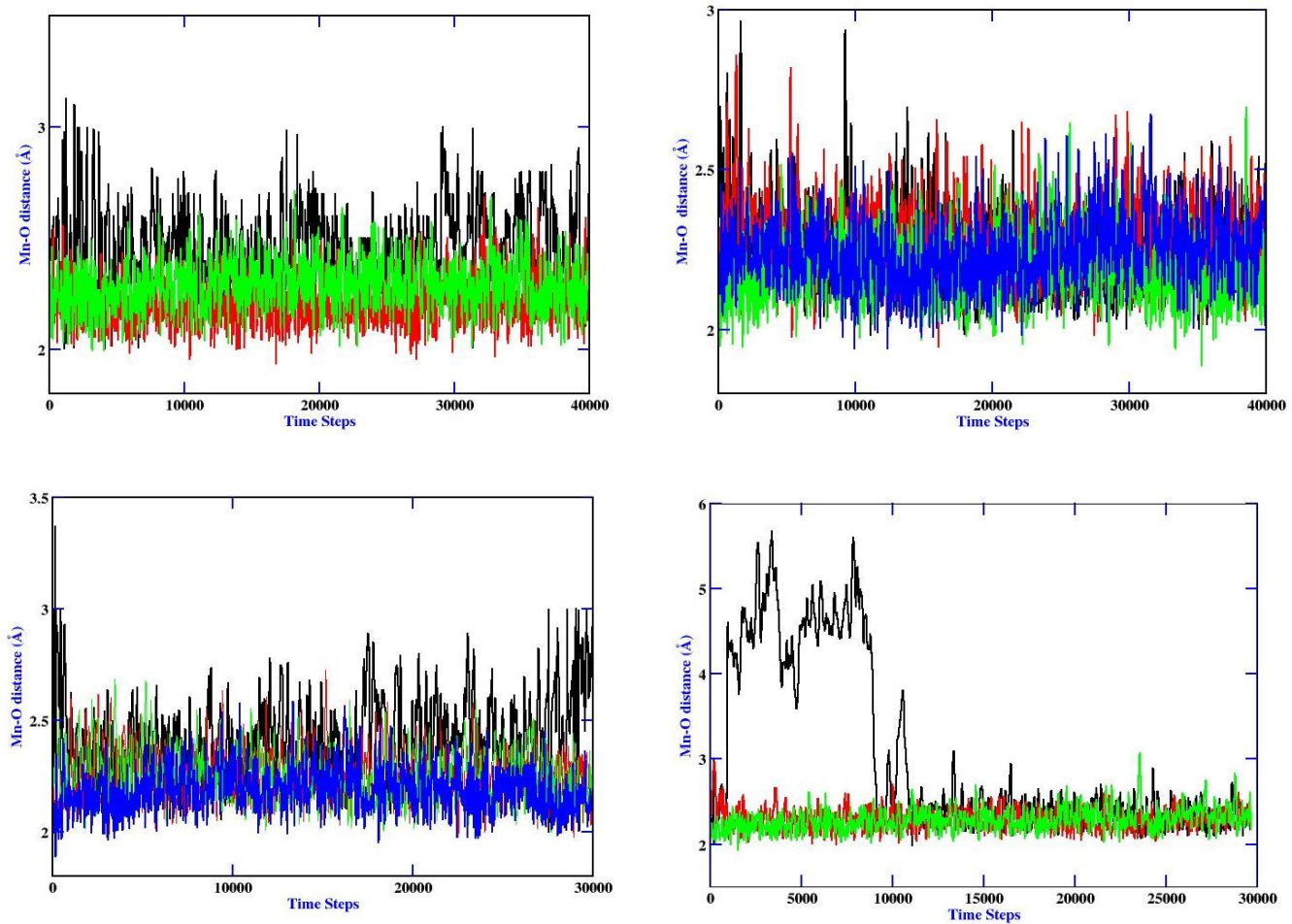


Figure S4: Plots of Mn-O bond distances, at 25°C during the AIMD trajectories of a) $[\text{Mn}(\text{dpasam})(\text{H}_2\text{O})]^{+}$ complex, b) $[\text{Mn}(\text{dpaaa})(\text{H}_2\text{O})]^{+}$ complex, c) $[\text{Mn}(\text{cbda})(\text{H}_2\text{O})]^{+}$ complex, d) $[\text{Mn}(\text{pydpa})(\text{H}_2\text{O})]$. Black, blue, red, and green curves represent the Mn-O distances for individual oxygen atoms along the AIMD trajectory.

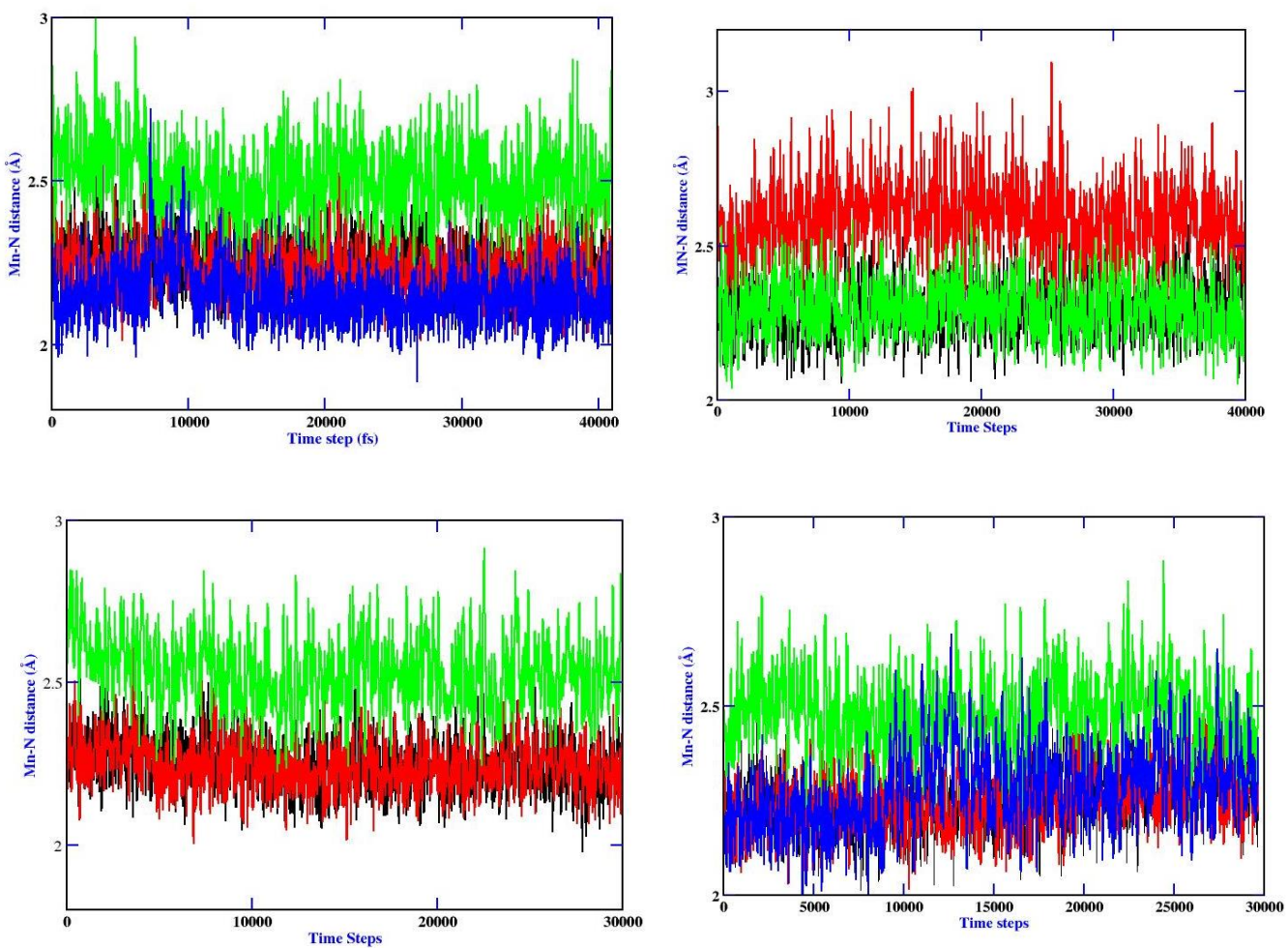


Figure S5: Plots of Mn-N bond distances, at 25°C during the AIMD trajectories of a) [Mn(dpasam)(H₂O)]⁻ complex, b) [Mn(dpaaa)(H₂O)]⁻ complex, c)[Mn(cbda)(H₂O)]⁻ complex, d) [Mn(pydpa)(H₂O)]⁻. Orange, blue, yellow, and grey curves represent the Mn-O distances for individual oxygen atoms along the AIMD trajectory.

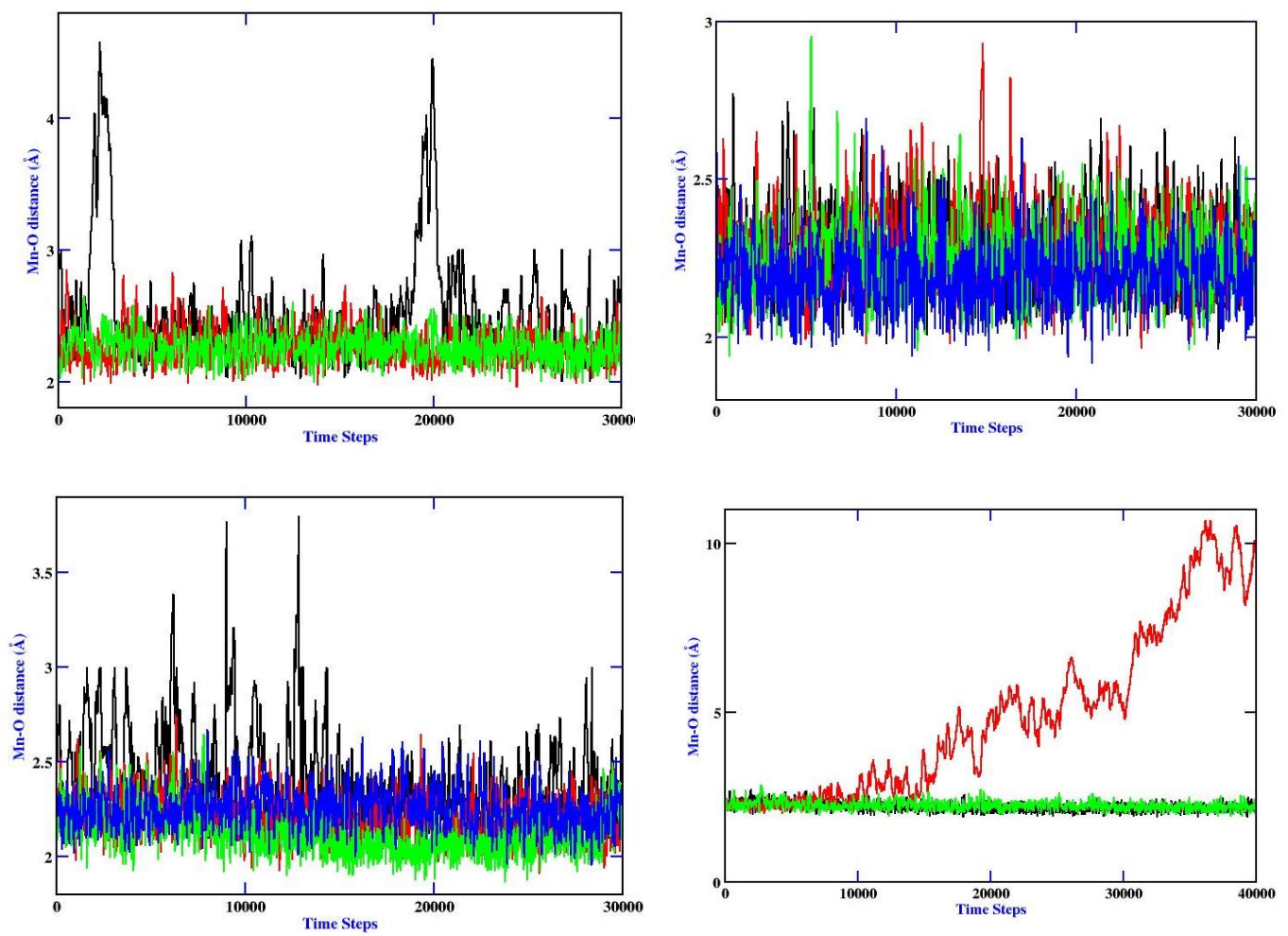


Figure S6: Plots of Mn-O bond distances, at 90°C during the AIMD trajectories of a) $[\text{Mn}(\text{dpasam})(\text{H}_2\text{O})]^{+}$ complex, b) $[\text{Mn}(\text{dpaaa})(\text{H}_2\text{O})]^{+}$ complex, c) $[\text{Mn}(\text{cbda})(\text{H}_2\text{O})]^{+}$ complex, d) $[\text{Mn}(\text{pydpa})(\text{H}_2\text{O})]$. Orange, blue, yellow, and grey curves represent the Mn-O distances for individual oxygen atoms along the AIMD trajectory.

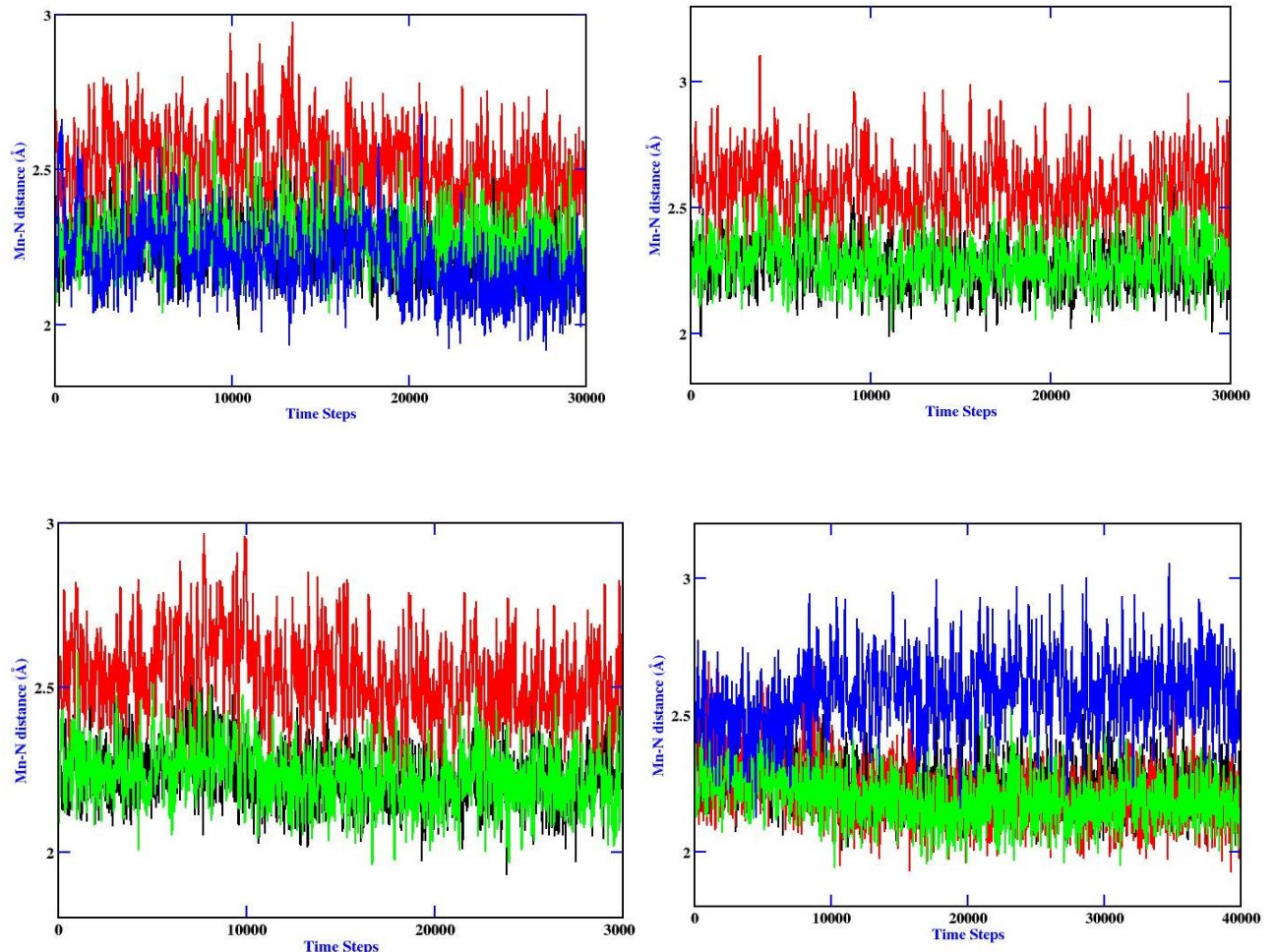


Figure S7: Plots of Mn-N bond distances, at 90°C during the AIMD trajectories of a) $[\text{Mn}(\text{dpasam})(\text{H}_2\text{O})]^-$ complex, b) $[\text{Mn}(\text{dpaaa})(\text{H}_2\text{O})]^-$ complex, c) $[\text{Mn}(\text{cbda})(\text{H}_2\text{O})]^-$ complex, d) $[\text{Mn}(\text{pydpa})(\text{H}_2\text{O})]$. Orange, blue, yellow, and grey curves represent the Mn-O distances for individual oxygen atoms along the AIMD trajectory.

Root mean square distance analysis

To calculate the root mean square distance (RMSD) of each simulation frame (2 ps interval) of the Mn(II) complexes trajectories to the ideal geometries, the first coordination spheres of each of the seven coordinated Mn(II) ions (7-coordinate) were compared against the crystallographic structure of each of the complexes.

Table S1: RMSD value of the structures was calculated at 2 ps intervals against the Crystal structure using discovery studio and Pymol (at 25⁰C).

25⁰C	Complex 1	Complex 2	Complex 3	Complex 4
Poses	RMSD	RMSD	RMSD	RMSD
14ps	0.328	0.394	0.322	0.277
16ps	0.324	0.420	0.311	0.275
18ps	0.310	0.301	0.540	0.397
20ps	0.418	0.531	0.430	0.435
22ps	0.496	0.396	0.530	0.317
24ps	0.518	0.418	0.590	0.426
26ps	0.310	0.353	0.499	0.437
28ps	0.505	0.368	0.411	0.527
30ps	0.300	0.314	0.548	0.518
32ps	0.499	0.399	0.239	0.533
34ps	0.327	0.315	0.346	0.421
36ps	0.410	0.355	0.540	0.321
38ps	0.433	0.433	0.344	0.324
40ps	0.460	0.401	0.344	0.513

Table S2: RMSD value of the structures was calculated at 2 ps intervals against the Crystal structure using discovery studio and Pymol (90⁰C).

90⁰C	Complex 1	Complex 2	Complex 3	Complex 4
Poses	RMSD	RMSD	RMSD	RMSD
14ps	0.228	0.290	0.296	0.340
16ps	0.124	0.420	0.500	0.575
18ps	0.184	0.280	0.526	0.697

20ps	0.085	0.491	0.450	0.535
22ps	0.097	0.496	0.239	0.620
24ps	0.090	0.245	0.437	0.630
26ps	0.139	0.453	0.465	0.773
28ps	0.340	0.268	0.429	0.727
30ps	0.460	0.310	0.340	0.790
32ps	0.100	0.285	0.445	0.733
34ps	0.255	0.300	0.555	0.755
36ps	0.201	0.306	0.554	0.721
38ps	0.312	0.355	0.510	0.720
40ps	0.311	0.467	0.465	0.729

Table S3: Bond length and bond angles of the Mn(II) complexes (temperature annealing+geometry optimization) with their crystallographic structure.

AIMD simulated structure	AIMD simulated bond length	X-ray Crystallographic bond length
[Mn(dpasam)(H ₂ O)] ⁻ (Complex 1)	Mn-O(w)=2.41	2.345
	Mn-O1=2.18	2.260
	Mn-O2=2.28	2.218
	Mn-N1=2.35	2.261
	Mn-N2=2.62	2.272
	Mn-N3=2.29	2.514
	Mn-N4=2.17	2.196
[Mn(dpaaa)(H ₂ O)] ⁻ (Complex 2)	Mn-O(w)=2.30	2.267
	Mn-O1=2.17	2.204
	Mn-O2=2.08	2.165
	Mn-O3=2.02	2.20
	Mn-N1=2.31	2.249
	Mn-N2=2.35	2.249
	Mn-N3=2.78	2.457
[Mn(cbda)(H ₂ O)] ⁻ (Complex 3)	Mn-O(w)=2.29	2.24
	Mn-O1=2.43	2.28

	Mn-O2=2.07	2.21
	Mn-O47=2.08	2.14
	Mn-N4=2.24	2.22
	Mn-N5=2.55	2.45
	Mn-N9=2.24	2.24
[Mn(pydpa)(H₂O)] (Complex 4)	Mn-O(w)=2.28	2.21
	Mn-O1=2.28	2.23
	Mn-O2=2.28	2.26
	Mn-N1=2.23	2.29
	Mn-N2=2.21	2.28
	Mn-N3=2.46	2.31
	Mn-N4=2.21	--

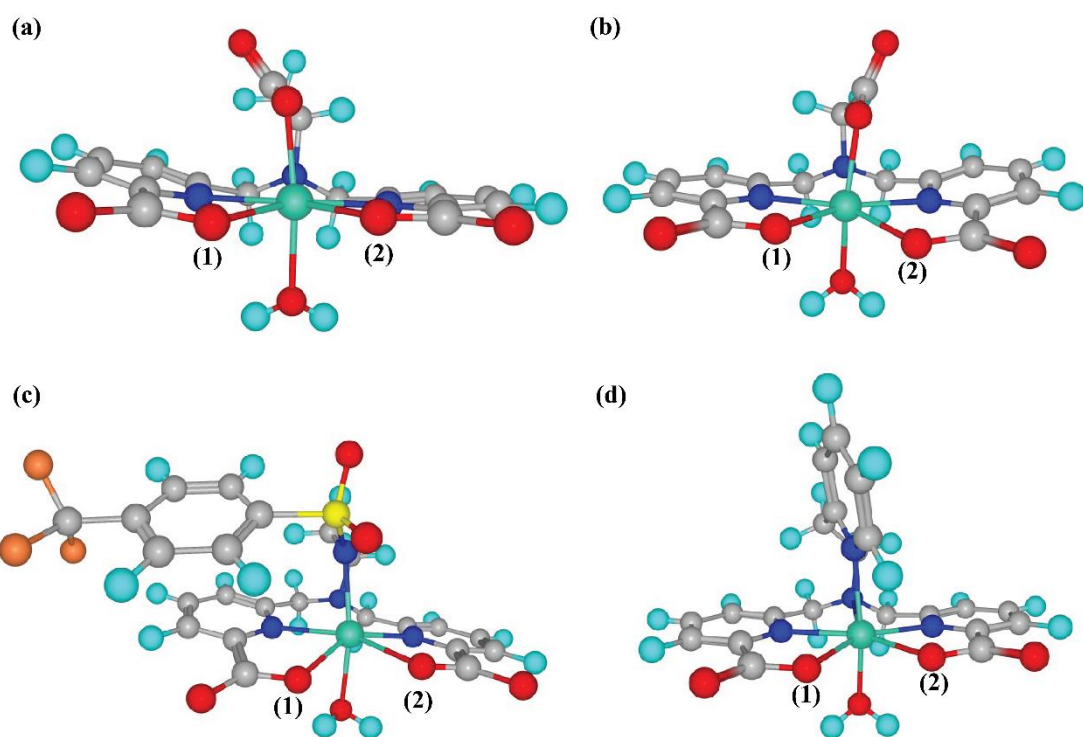


Figure S8: The Optimized structure of all four complexes using PBE/DZVP with GTH pseudopotential a) $[\text{Mn}(\text{dpasam})(\text{H}_2\text{O})]^-$, b) $[\text{Mn}(\text{dpaaa})(\text{H}_2\text{O})]^-$, c) $[\text{Mn}(\text{cbda})(\text{H}_2\text{O})]^-$, and d) $[\text{Mn}(\text{pydpa})(\text{H}_2\text{O})]$. Only the water molecule directly connected to the metal center is shown.

Table S4: Binding energy values and relative binding energy (ΔE_{REL}) values (in kcal mol⁻¹) of the chosen complexes at 25°C.

	Complex	ΔE_{total}	$\Delta E_{\text{relative}}$
M06-2X/def2-TZVP	[Mn(dpasam)(H ₂ O)] ⁺	-152.009	0.000
	[Mn(dpaaaa)(H ₂ O)] ⁺	-150.942	+1.066
	[Mn(cbda)(H ₂ O)] ⁻	-146.047	+5.962
	[Mn(pydpa)(H ₂ O)]	-130.799	+21.210
M06/def2-TZVP	[Mn(dpasam)(H ₂ O)] ⁺	-139.980	0.000
	[Mn(dpaaaa)(H ₂ O)] ⁺	-138.410	+1.570
	[Mn(cbda)(H ₂ O)] ⁻	-131.760	+8.220
	[Mn(pydpa)(H ₂ O)]	-117.141	+22.840

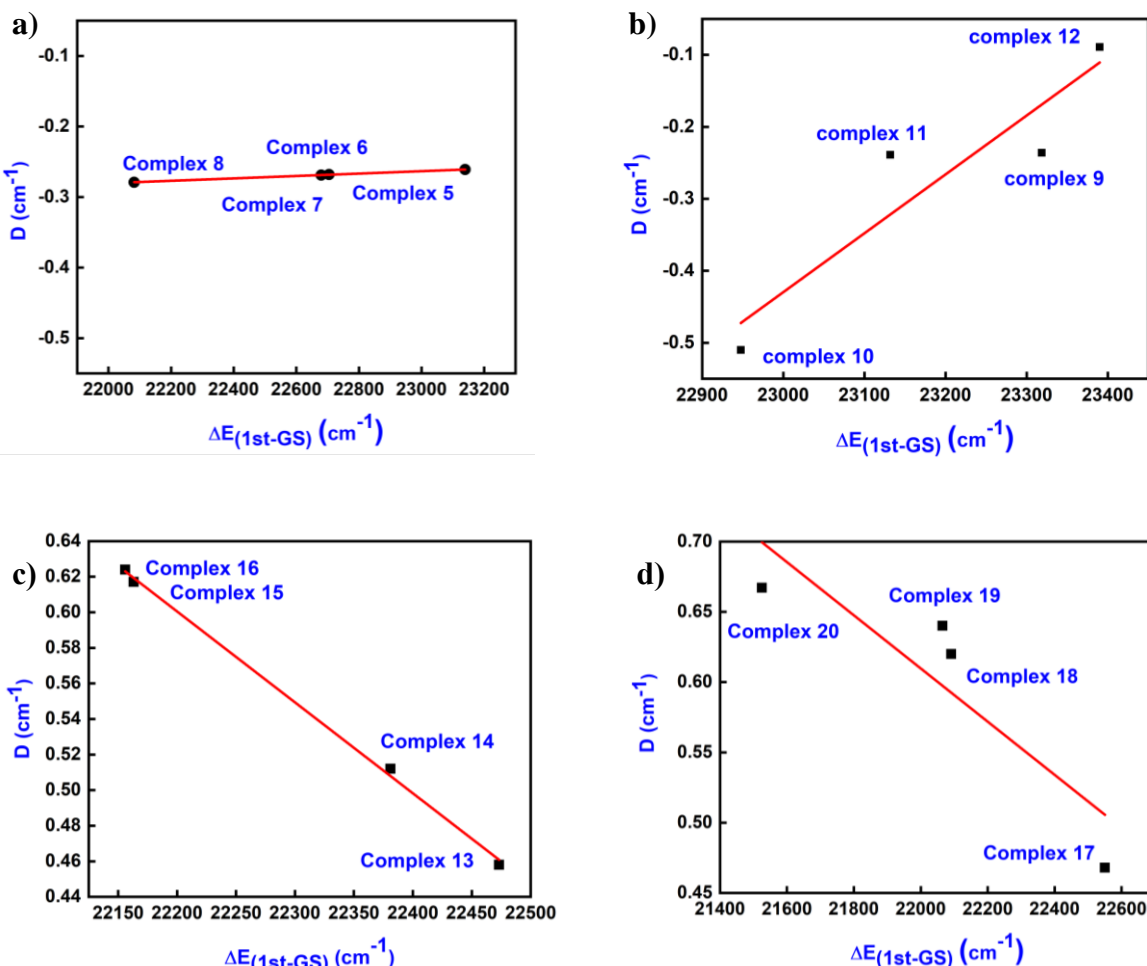


Figure S9: Variation of D values of Class II (a, b) and Class III (c, d) complexes with the energy difference between the ground and first excited $\Delta E_{(1\text{st-GS})}$. The solid line serves only as a guide for the eye.

Table S5: Spin–Orbit Coupling (SOC) and Spin–Spin (SS) Contributions to the D Values (cm^{-1}) Calculated using TPSS/def2-TZVP level of theory.

Complexes	Dsoc	Dss	$\alpha \rightarrow \alpha$	$\beta \rightarrow \beta$	$\alpha \rightarrow \beta$	$\beta \rightarrow \alpha$
Complex 1	-0.0890	-0.0096	-0.0595	-0.04784	-0.0437	0.0620
Complex 2	-0.02141	-0.01268	-0.06638	-0.07527	0.08127	0.03897
Complex 3	-0.01829	-0.01265	-0.06600	-0.07351	0.08370	0.03753
Complex 4	-0.03750	-0.01272	-0.043322	-0.06051	0.03857	0.02767
Complex 5	-0.04001	-0.01407	-0.06241	-0.07318	0.05771	0.03788
Complex 6	-0.04098	-0.01200	-0.05909	-0.07136	0.05174	0.03773
Complex 7	-0.04071	-0.01125	-0.06399	-0.07593	0.05827	0.04093
Complex 8	-0.06284	-0.01322	-0.04206	-0.06122	0.01299	0.02746
Complex 9	0.08778	0.02158	0.01741	0.00571	0.12346	-0.05881
Complex 10	-0.09605	-0.00719	0.03622	0.01212	-0.16634	0.02195
Complex 11	-0.09553	-0.00716	0.03164	0.01026	-0.16106	0.02362
Complex 12	-0.13595	-0.00018	0.01182	-0.03645	-0.15772	0.04641
Complex 13	-0.02220	-0.01803	-0.09060	-0.09409	0.11476	0.04773
Complex 14	-0.04098	-0.01200	-0.05909	-0.07136	0.05174	0.03773
Complex 15	0.03052	-0.00120	0.03718	0.04479	-0.02810	-0.2334
Complex 16	-0.02636	-0.01385	-0.03495	-0.05339	0.03622	0.02575
Complex 17	-0.02526	-0.01959	-0.09765	-0.09941	0.12118	0.05063
Complex 18	-0.02131	-0.01313	-0.06686	-0.07537	0.08200	0.03892
Complex 19	-0.01955	-0.01291	-0.06529	-0.07203	0.08079	0.03698
Complex 20	-0.04452	-0.01159	-0.03858	-0.05646	0.02392	0.02660

Table S6: Spin–Orbit Coupling (SOC) and Spin–Spin (SS) Contributions to the D Values (cm^{-1}) Calculated using M06-2X/def2-TZVP level of theory.

Complexes	Dsoc	Dss	$\alpha \rightarrow \alpha$	$\beta \rightarrow \beta$	$\alpha \rightarrow \beta$	$\beta \rightarrow \alpha$
Complex 1	-0.0898	0.0097	-0.06795	-0.08784	0.0320	0.0339
Complex 2	-0.04610	-0.00727	-0.06191	-0.06684	0.04442	0.03824
Complex 3	-0.03611	-0.00716	-0.06106	-0.06563	0.05317	0.03742
Complex 4	0.05551	-0.00545	0.01828	0.02278	0.02641	-0.01196

Complex 5	-0.05702	-0.00279	-0.04719	-0.05226	0.00847	0.03395
Complex 6	-0.06511	-0.00174	-0.04254	-0.04797	-0.00768	0.03308
Complex 7	-0.06634	-0.00100	-0.04582	-0.05144	-0.00451	0.03543
Complex 8	-0.04641	-0.00466	-0.03246	-0.03793	0.00542	0.01856
Complex 9	0.82227	0.00769	-0.07288	-0.04800	1.00238	-0.05924
Complex 10	0.26146	0.00450	-0.14312	-0.11221	0.49681	0.01998
Complex 11	0.55327	0.00316	0.01191	0.05127	0.49077	-0.00068
Complex 12	0.43541	-0.00912	0.07569	0.10770	0.31640	-0.06438
Complex 13	0.03602	-0.00641	0.00048	0.00198	0.03942	-0.00586
Complex 14	-0.06511	-0.00174	-0.04254	-0.04797	-0.00768	0.03308
Complex 15	0.08329	-0.00156	0.05552	0.05788	-0.00303	-0.02708
Complex 16	0.04303	-0.00720	0.02063	0.02339	0.01395	-0.01494
Complex 17	-1.45354	-0.25733	-0.54602	-0.08216	-0.86231	0.03695
Complex 18	-0.04144	-0.00673	-0.05701	-0.06227	0.04037	0.03748
Complex 19	-0.03992	-0.00676	-0.06154	-0.06661	0.04941	0.03882
Complex 20	0.05551	-0.00545	0.01828	0.02278	0.02641	-0.01196

Table S7: ZFS parameter of all the complexes using M06-2X/def2-TZVP.

Complexes	D (cm ⁻¹)	E/D	Δ (cm ⁻¹)	Δ ² (10 ²⁰ s ⁻²)
Complex 1	-0.0995	0.1044	0.0826	2.4209
Complex 2	-0.0537	0.1017	0.0445	0.7039
Complex 3	-0.0429	0.1839	0.0369	0.4822
Complex 4	0.0499	0.1550	0.0422	0.6323
Complex 5	-0.0597	0.0358	0.0530	0.9980
Complex 6	-0.0667	0.2053	0.0578	1.1850
Complex 7	-0.0672	0.2171	0.0586	1.2198
Complex 8	-0.0509	0.2497	0.0454	0.7299
Complex 9	0.8299	0.0357	0.6789	163.7102
Complex 10	0.2659	0.2334	0.2342	19.4848
Complex 11	0.5564	0.0702	0.4577	74.3959
Complex 12	0.4263	0.0973	0.3529	44.2548
Complex 13	0.0297	0.2796	0.0269	0.2575

Complex 14	-0.0666	0.2053	0.0577	1.1831
Complex 15	0.0815	0.0924	0.0674	1.6132
Complex 16	0.0356	0.2536	0.0317	0.3572
Complex 17	-0.0561	0.2400	0.0496	0.8739
Complex 18	-0.0479	0.2491	0.0426	0.6437
Complex 19	-0.0464	0.0195	0.0379	0.5096
Complex 20	0.0473	0.1374	0.0397	0.5602

Table S8: NEVPT2 transition energy and their individual contribution to the D values for Complex 1 (up to 17 quartets and 13 doublets are shown).

Complex 1	NEVPT2 Transition energies	D (cm ⁻¹)	Major CASSCF electronic Wave function $d_{yz}d_{xz}d_x^2-y^2d_{xy}d_z^2$	E (cm ⁻¹)
⁶ S	0.000	0.000	1 1 1 1 1	0.000
⁴ G	22576.1	0.454	0 2 1 1 1 (37%)	0.044
	23065.7	-0.164	0 1 2 1 1 (38%)	0.166
	25126.9	-0.130		-0.131
	26544.1	-0.012		-0.009
	26776.7	-0.000		-0.002
	27226.1	-0.001		-0.000
	27606.8	-0.000		0.000
	27710.5	-0.000		-0.000
	27811.4	-0.000		0.000
⁴ P	31139.5	-0.448	1 1 1 0 2 (52%)	-0.388
	31848.8	-0.053		0.055
	32085.3	0.142		-0.008
⁴ D	32346.2	-0.009		-0.009
	33360.6	-0.192		0.153
	33865.5	0.215		0.034
	34441.3	-0.236		0.104
	35316.5	0.464	2 0 1 1 1 (22%)	-0.004
² I	32691.3	0.000		0.000

	34545.6	0.000		0.000
	34772.2	0.000		0.000
	35815.8	0.000		0.000
	36542.4	0.000		0.000
	36976.9	0.000		0.000
	37114.0	0.000		0.000
	37829.1	0.000		0.000
	38836.8	0.000		0.000
	39297.3	0.000		0.000
	39548.1	0.000		0.000
	39596.8	0.000		0.000
	39954.5	0.000		0.000

Table S9: NEVPT2 transition energy and their individual contribution to the D values for Complex 2 (up to 17 quartets and 13 doublets are shown).

Complex 2	NEVPT2 Transition energies	D (cm ⁻¹)	Major CASSCF electronic Wave function $d_{xz}d_{yz}d_{x^2-y^2}d_{xy}d_z^2$	E(cm ⁻¹)
⁶ S	0.000	0.000	1 1 1 1 1	0.000
⁴ G	22142.4	0.643	2 1 1 1 0 (66%)	-0.012
	23110.8	-0.274	1 2 1 1 0 (53%)	0.269
	25199.9	-0.164		-0.173
	26560.3	-0.0003		-0.007
	26755.4	-0.002		0.001
	27212.2	-0.000		0.000
	27774.2	-0.000		0.000
	27828.2	-0.000		0.000
	27861.6	-0.000		0.000
⁴ P	31144.1	-0.043	1 1 0 2 1 (55%)	0.019
	31919	-0.432		-0.422

	32373.5	0.053		-0.080
⁴D	32389.9	-0.003		0.003
	33588.6	-0.223		0.222
	33744.3	-0.017		-0.056
	34495.7	-0.265		0.262
	36036.1	0.760	0 1 1 1 2 (42%)	-0.025
²I	32290.5	0.000		0.000
	33527.7	0.000		0.000
	35084.7	0.000		0.000
	35563.6	0.000		0.000
	36330.8	0.000		0.000
	36812.4	0.000		0.000
	36981.7	0.000		0.000
	37922.0	0.000		0.000
	38893.3	0.000		0.000
	39060.8	0.000		0.000
	39547.2	0.000		0.000
	39805.9	0.000		0.000
	39919.3	0.000		0.000

Table S10: NEVPT2 transition energy and their individual contribution to the D values for Complex 3 (up to 17 quartets and 13 doublets are shown).

Complex 3	NEVPT2 Transition energies	D (cm ⁻¹)	Major CASSCF electronic Wave function $d_{xz}d_{yz}d_{x^2-y^2}d_{xy}d_z^2$	E (cm ⁻¹)
⁶S	0.000	0.000	1 1 1 1 1	0.000
⁴G	22165.4	0.636	1 0 1 1 2 (53%)	0.012
	23122.3	-0.275	1 0 1 2 1 (49%)	-0.227
	24978.8	-0.174		0.155

	26568.3	-0.001		0.003
	26773.4	-0.001		-0.000
	27154.5	-0.000		-0.000
	27783.6	-0.000		-0.000
	27836.9	-0.000		-0.000
	27871.0	-0.026		-0.000
⁴P	31219.2	-0.333	1 1 0 2 1 (40%)	0.256
	32289.3	-0.039		0.138
	32382.3	-0.003		-0.001
⁴D	33595.1	-0.239		-0176
	33798.0	-0.020		-0.066
	34467.3	-0.245		-0.226
	35998.1	0.750	1 1 2 1 0 (42%)	-0.012
	44952.6	-0.001		0.005
²I	32273.4	0.000		0.000
	33304.0	0.000		0.000
	34857.9	0.000		0.000
	35722.6	0.000		0.000
	36338.9	0.000		0.000
	36876.1	0.000		0.000
	36951.3	0.000		0.000
	37935.8	0.000		0.000
	38708.9	0.000		0.000
	38927.6	0.000		0.000
	39462.0	0.000		0.000
	39776.1	0.000		0.000

Table S11: NEVPT2 transition energy and their individual contribution to the D values for Complex 4 (up to 17 quartets and 13 doublets are shown).

Complex 4	NEVPT2 Transition energies	D (cm ⁻¹)	Major CASSCF electronic Wave function $d_{yz}d_{xz}d_{x^2-y^2}d_{xy}d_z^2$	E (cm ⁻¹)
⁶ S	0.000	0.000	1 1 1 1 1	0.000
⁴ G	21692.4	0.716	0 1 1 2 1 (50%)	-0.000
	22430.0	-0.303	0 2 1 1 1 (47%)	0.292
	25387.1	-0.109		-0.107
	26092.9	-0.032		-0.032
	26288.6	-0.029		-0.019
	27335.0	-0.000		-0.000
	27689.7	-0.000		-0.000
	27743.1	-0.000		-0.000
	27819.4	-0.000		0.000
⁴ P	30374.4	-0.056		0.046
	31101.0	-0.076		-0.150
	32169.3	-0.382	1 1 2 1 0 (42%)	-0.404
⁴ D	32636.6	0.000		0.000
	33397.6	-0.002		0.002
	33589.8	-0.050		-0.045
	35274.4	-0.444		0.422
	36445.4	0.803	2 1 1 0 1 (31%)	-0.002
² I	31079.5	0.000		0.000
	33644.0	0.000		0.000
	34221.6	0.000		0.000
	34761.7	0.000		0.000
	35855.3	0.000		0.000
	36343.8	0.000		0.000
	36391.7	0.000		0.000
	37248.9	0.000		0.000

	39132.1	0.000		0.000
	39235.6	0.000		0.000
	39273.7	0.000		0.000
	39466.0	0.000		0.000
	39554.7	0.000		0.000

Table S12: NEVPT2 transition energy and their individual contribution to the D values for Complex 5 (up to 17 quartets and 13 doublets are shown).

Complex 5	NEVPT2 Transition energies	D (cm ⁻¹)	Major CASSCF electronic Wave function $d_{yz}d_{xz}d_x^2-y^2d_{xy}d_z^2$	E (cm ⁻¹)
⁶ S	0.000	0.000	1 1 1 1 1	0.000
⁴ G	23139.6	-0.261	2 1 1 0 1 (82%)	-0.100
	23571.7	-0.248	1 2 1 0 1 (43%)	0.081
	26792.8	0.034		0.000
	26989.8	0.000		-0.000
	27277.8	-0.000		0.000
	27373.7	0.000		0.000
	27407.6	0.018		0.000
	27533.2	0.000		0.000
	27599.0	0.000		-0.000
⁴ P	30518.6	1.452	1 2 0 1 1 (24%)	0.018
	31775.8	-0.013		0.018
	32178.5	-0.151		-0.147
⁴ D	32940.7	-0.110		0.136
	32954.1	-0.100		-0.025
	33236.4	-0.279	1 0 2 1 1 (43%)	0.278
	33240.5	-0.127		-0.059
	34000.9	-0.237		-0.204

Table S13: NEVPT2 transition energy and their individual contribution to the D values for Complex 6 (up to 17 quartets and 13 doublets are shown).

Complex 6	NEVPT2 Transition energies	D (cm⁻¹)	Major CASSCF electronic Wave function d_{xz}d_{yz}d_{x²-y²}d_{xy}d_{z²}	E (cm⁻¹)
⁶S	0.000	0.000	1 1 1 1 1	0.000
⁴G	22704.6	-0.268	2 1 1 1 0 (55%)	0.210
	23025.4	-0.280	1 2 1 1 0 (46%)	-0.206
	26650.5	0.055		0.000
	26952.1	0.000		0.000
	27158.9	0.004		0.000
	27316.7	0.003		0.000
	27354.6	0.022		0.000
	27522.5	-0.000		-0.000
	27666.9	0.000		-0.000
⁴P	30705.2	1.418	1 1 0 2 1 (55%)	0.020
	31735.5	-0.004		-0.007
	31871.5	-0.039		-0.015
⁴D	32368.9	-0.001		-0.000
	32920.5	-0.095		-0.069
	33159.0	-0.138		-0.132
	34185.9	-0.431	0 1 1 1 2 (46%)	0.457
	34601.5	-0.268		-0.263

Table S14: NEVPT2 transition energy and their individual contribution to the D values for Complex 7 (up to 17 quartets and 13 doublets are shown).

Complex 7	NEVPT2 Transition energies	D (cm ⁻¹)	Major CASSCF electronic Wave function $d_{yz}d_{xz}d_{x^2-y^2}d_{xy}d_z^2$	E (cm ⁻¹)
⁶S	0.000	0.000	1 1 1 1 1	0.000
⁴G	22679.5	-0.269	0 1 1 2 1 (55%)	-0.281
	22996.0	-0.280	1 1 0 2 1 (72%)	-0.275
	26717.0	0.047		0.000
	26960.2	0.000		0.000
	27126.1	0.007		0.000
	27308.7	0.005		0.000
	27336.0	0.021		0.000
	27524.3	-0.000		-0.000
	27660.9	0.000		-0.000
4p	30701.2	1.421	0 2 1 1 1 (59%)	0.022
	31794.6	-0.002		-0.006
	31873.0	-0.023		-0.019
⁴D	32312.9	-0.002		-0.003
	32978.1	-0.133		-0.127
	33047.5	-0.116		-0.093
	34197.9	-0.438	1 2 0 1 1 (30%)	0.472
	34600.6	-0.263	2 1 0 1 1 (53%)	-0.258

Table S15: NEVPT2 transition energy and their individual contribution to the D values for Complex 8 (up to 17 quartets and 13 doublets are shown).

Complex 8	NEVPT2 Transition energies	D (cm ⁻¹)	Major CASSCF electronic Wave function $d_{xz}d_{yz}d_{x^2-y^2}d_{xy}d_z^2$	E (cm ⁻¹)
⁶S	0.000	0.000	1 1 1 1 1	0.000
⁴G	22082.1	-0.279	1 2 1 0 1 (69%)	-0.144
	22189.5	-0.240	2 1 1 0 1 (63%)	0.138
	26425.4	0.010		0.000
	26511.1	-0.000		-0.000
	27249.8	0.000		0.000
	27338.6	0.000		-0.000
	27426.1	0.015		0.000
	27542.7	0.000		0.000
	27620.1	0.001		-0.000
⁴P	30386.6	1.333	0 2 1 1 1 (42%)	0.000
	30945.1	-0.033		0.011
	31159.4	-0.045		-0.016
⁴D	32567.5	0.002		0.000
	32725.9	0.009		-0.001
	33132.4	-0.017		0.005
	35171.4	-0.394	2 1 0 1 1 (50%)	0.394
	35405.4	-0.391	0 1 1 1 2 (26%)	-0.390

Table S16: NEVPT2 transition energy and their individual contribution to the D values for Complex 9 (up to 17 quartets and 13 doublets are shown).

Complex 9	NEVPT2 Transition energies	D (cm ⁻¹)	Major CASSCF electronic Wave function $d_{yz}d_{xz}d_{x^2-y^2}d_{xy}d_z^2$	E (cm ⁻¹)
⁶S	0.000	0.000	1 1 1 1 1	0.000
⁴G	23318.6	-0.236	2 1 1 1 0 (45%)	-0.097
	23977.3	-0.222	1 2 1 1 0 (56%)	0.110
	27172.0	0.013		-0.000
	27253.8	0.000		0.000
	27391.0	0.002		0.000
	27410.3	0.001		0.000
	27636.0	0.001		-0.000
	27669.7	-0.000		0.000
	27708.8	1.340	1 1 0 2 1 (51%)	-0.070
⁴P	30430.5	-0.181		0.068
	32567.2	-0.146		0.055
	32714.8	0.015		0.005
⁴D	32789.3	-0.028		0.019
	32852.9	-0.188		0.084
	32913.1	-0.208	1 0 1 1 2 (21%)	-0.222
	33152.5	-0.189		0.043
	33907.2	0.000		0.000

Table S17: NEVPT2 transition energy and their individual contribution to the D values for Complex 10 (up to 17 quartets and 13 doublets are shown).

Complex 10	NEVPT2 Transition energies	D (cm⁻¹)	Major CASSCF electronic Wave function d_{xz}d_{yz}d_{x²-y²}d_{xy}d_{z²}	E (cm⁻¹)
⁶S	0.000	0.000	1 1 1 1 1	0.000
⁴G	22947.6	-0.510	1 2 1 1 0 (41%)	-0.013
	23187.5	0.266	2 1 1 1 0 (41%)	0.264
	26915.0	0.015		-0.014
	27084.4	0.004		-0.005
	27193.9	0.002		-0.002
	27308.1	0.001		-0.001
	27461.8	0.004		-0.004
	27568.8	0.000		0.000
	27692.5	0.000		-0.000
⁴P	30505.7	0.605	1 1 0 2 1 (44%)	-0.688
	32266.2	-0.029		0.002
	32331.5	-0.000		-0.010
⁴D	32543.0	0.101		0.107
	32638.7	0.008		0.069
	33101.3	-0.050		0.173
	33934.7	-0.332	0 1 1 1 2 (47%)	0.019
	34088.6	-0.110		0.069

Table S18: NEVPT2 transition energy and their individual contribution to the D values for Complex 11 (up to 17 quartets and 13 doublets are shown).

Complex 11	NEVPT2 Transition energies	D (cm ⁻¹)	Major CASSCF electronic Wave function $d_{xz}d_{yz}d_{x^2-y^2}d_{xy}d_z^2$	E (cm ⁻¹)
⁶S	0.000	0.000	1 1 1 1 1	0.000
⁴G	23132.0	-0.239	1 1 0 1 2 (45%)	-0.256
	23317.0	-0.267	0 1 1 2 1 (48%)	0.260
	27010.0	0.024		0.000
	27164.6	0.016		-0.000
	27282.4	0.004		0.000
	27390.4	0.001		-0.000
	27548.6	0.009		-0.000
	27649.3	-0.000		-0.000
	27769.4	0.000		0.000
⁴P	30598.8	1.371	0 1 2 1 1 (42%)	-0.034
	32319.3	-0.032		-0.033
	32498.1	-0.002		-0.003
⁴D	32528.6	-0.127		0.126
	32850.6	-0.009		-0.002
	33101.9	-0.125		0.045
	33937.1	-0.426	1 0 2 1 1 (52%)	-0.198
	34121.2	-0.223		0.087

Table S19: NEVPT2 transition energy and their individual contribution to the D values for Complex 12 (up to 17 quartets and 13 doublets are shown).

Complex 12	NEVPT2 Transition energies	D (cm ⁻¹)	Major CASSCF electronic Wave function $d_{yz}d_{xz}d_{x^2-y^2}d_{xy}d_z^2$	E (cm ⁻¹)
⁶ S	0.000	0.000	1 1 1 1 1	0.000
⁴ G	23390.0	-0.089	2 1 1 1 0 (62%)	-0.174
	24107.6	-0.173	1 2 1 1 0 (36%)	0.131
	26375.4	0.064		0.004
	26813.9	0.002		-0.000
	27280.4	0.005		0.001
	27489.1	-0.000		0.001
	27543.4	0.000		0.000
	27582.2	-0.000		-0.000
	27685.4	0.001		0.000
⁴ P	30827.5	0.756	1 1 0 2 1 (40%)	0.049
	31772.4	-0.179	1 2 0 1 1 (32%)	0.159
	31879.7	-0.062		-0.064
⁴ D	33083.2	-0.209	1 0 1 1 2 (14%)	0.037
	33171.4	-0.111		-0.097
	33290.5	-0.040		0.040
	33342.0	-0.017		0.008
	34217.0	0.020		-0.099

Table S20: NEVPT2 transition energy and their individual contribution to the D values for Complex 13 (up to 17 quartets and 13 doublets are shown).

Complex 13	NEVPT2 Transition energies	D (cm ⁻¹)	Major CASSCF electronic Wave function $d_{yz}d_{xz}d_{x^2-y^2}d_{xy}d_z^2$	E (cm ⁻¹)
⁶ S	0.000	0.000	1 1 1 1 1	0.000
⁴ G	22473.2	0.458	2 1 1 0 1 (47%)	0.042
	22985.3	-0.176	2 1 1 0 1 (39%)	0.162
	24983.7	-0.137		-0.135
	26464.7	-0.010		-0.007
	26751.5	0.001		-0.001
	27174.4	-0.001		-0.000
	27603.2	-0.000		0.000
	27702.5	-0.000		-0.000
	27800.0	-0.000		0.000
⁴ P	31104.0	-0.422	2 1 0 1 1 (60%)	-0.352
	31838.3	-0.050		0.050
	32127.9	0.126		-0.013
⁴ D	32284.6	-0.013		-0.009
	33365.8	-0.199		0.147
	33915.9	0.219		0.029
	34467.8	-0.247		0.100
	35357.7	0.472	1 0 2 1 1 (26%)	-0.006

Table S21: NEVPT2 transition energy and their individual contribution to the D values for Complex 14 (up to 17 quartets and 13 doublets are shown).

Complex 14	NEVPT2 Transition energies	D (cm ⁻¹)	Major CASSCF electronic Wave function $d_{xz}d_{yz}d_{x^2-y^2}d_{xy}d_z^2$	E (cm ⁻¹)
⁶ S	0.000	0.000	1 1 1 1 1	0.000
⁴ G	22381.1	0.512	2 1 1 1 0 (57%)	-0.004
	23196.6	-0.262	1 2 1 1 0 (47%)	-0.063
	25083.4	-0.188		0.044
	26465.6	-0.006		0.002
	26750.4	-0.003		0.003
	27274.7	-0.000		0.000
	27774.8	-0.000		-0.000
	27827.3	-0.000		-0.000
	27856.9	-0.000		-0.000
⁴ P	31139.0	-0.060		-0.061
	31872.5	0.187		0.018
	32473.2	-0.434	1 1 0 2 1 (49%)	0.160
⁴ D	32498.7	-0.001		0.000
	33618.5	-0.209		-0.022
	33757.0	-0.070		0.051
	34406.5	-0.267		-0.127
	35832.5	0.823	0 1 1 1 2 (39%)	0.000

Table S22: NEVPT2 transition energy and their individual contribution to the D values for Complex 15 (up to 17 quartets and 13 doublets are shown).

Complex 15	NEVPT2 Transition energies	D (cm ⁻¹)	Major CASSCF electronic Wave function $d_{xz}d_{yz}d_{x^2-y^2}d_{xy}d_z^2$	E (cm ⁻¹)
⁶ S	0.000	0.000	1 1 1 1 1	0.000
⁴ G	22163.3	0.617	1 2 1 0 1 (80%)	0.016
	22649.8	-0.272	2 1 1 0 1 (76%)	-0.259
	23412.5	-0.201		0.235
	26197.3	0.002		-0.000
	26546.7	-0.000		0.001
	26661.5	-0.001		-0.000
	27203.8	-0.000		-0.000
	27637.7	-0.000		0.000
	27882.3	-0.000		-0.000
⁴ P	31076.9	-0.003		-0.001
	31754.9	-0.257		0.250
	32075.3	0.066		0.055
⁴ D	32398.9	-0.043		0.019
	33478.3	-0.330	0 1 1 2 1 (39%)	-0.318
	33897.7	-0.201		-0.200
	34403.1	0.000		0.150
	35744.4	0.646	1 1 2 1 0 (22%)	0.063

Table S23: NEVPT2 transition energy and their individual contribution to the D values for Complex 16 (up to 17 quartets and 13 doublets are shown).

Complex 16	NEVPT2 Transition energies	D (cm ⁻¹)	Major CASSCF electronic Wave function $d_{yz}d_{xz}d_{x^2-y^2}d_{xy}d_z^2$	E (cm ⁻¹)
⁶S	0.000	0.000	1 1 1 1 1	0.000
⁴G	22156.6	0.624	2 1 1 0 1 (46%)	-0.011
	22776.6	-0.276	1 2 1 0 1 (42%)	0.274
	25252.8	-0.086		-0.093
	26164.0	-0.017		-0.009
	26364.5	-0.039		-0.044
	27426.7	-0.000		0.000
	27644.5	-0.000		-0.000
	27666.6	-0.000		0.000
	27795.3	-0.000		0.000
⁴P	30342.2	-0.079		0.072
	31203.5	0.034		-0.073
	32027.1	-0.392		-0.472
⁴D	32770.0	-0.007		0.008
	33294.8	-0.080		0.082
	33559.8	0.001		-0.049
	34995.0	-0.348	1 0 1 2 1 (19%)	0.344
	36010.0	0.692	0 1 1 2 1 (24%)	-0.023

Table S24: NEVPT2 transition energy and their individual contribution to the D values for Complex 17 (up to 17 quartets and 13 doublets are shown).

Complex 17	NEVPT2 Transition energies	D (cm ⁻¹)	Major CASSCF electronic Wave function $d_{yz}d_{xz}d_x^2-y^2d_{xy}d_z^2$	E (cm ⁻¹)
⁶S	0.000	0.000	1 1 1 1 1	0.000
⁴G	22550.4	0.468	1 2 1 1 0 (48%)	0.036
	23076.5	-0.180	2 1 1 1 0 (49%)	0.176
	25153.7	-0.123		-0.129
	26560.7	-0.012		-0.010
	26764.7	-0.000		-0.003
	27235.3	-0.001		-0.000
	27591.8	-0.000		0.000
	27701.6	-0.000		-0.000
	27800.9	-0.000		0.000
⁴P	31107.1	-0.452	1 1 0 2 1 (36%)	-0.396
	31838.2	-0.055		0.058
	32023.9	0.148		-0.009
⁴D	32361.2	-0.010		-0.010
	33314.0	-0.196		0.159
	33815.5	0.220		0.025
	34454.7	-0.235		0.115
	35341.1	0.458	1 0 1 1 2 (29%)	-0.006

Table S25: NEVPT2 transition energy and their individual contribution to the D values for Complex 18 (up to 17 quartets and 13 doublets are shown).

Complex 18	NEVPT2 Transition energies	D (cm ⁻¹)	Major CASSCF electronic Wave function $d_{yz}d_{xz}d_x^2-y^2d_{xy}d_z^2$	E (cm ⁻¹)
⁶S	0.000	0.000	1 1 1 1 1	0.000
⁴G	22091.2	0.620	2 1 1 1 0 (65%)	-0.007
	23115.6	-0.273	1 2 1 1 0 (52%)	0.244
	25182.9	-0.170		-0.164
	26550.1	-0.002		-0.005
	26751.8	-0.002		0.001
	27196.9	-0.000		0.000
	27770.0	-0.000		0.000
	27823.5	-0.000		0.000
	27855.0	-0.000		0.000
⁴P	31142.9	-0.033		0.030
	31906.6	-0.445	1 1 0 2 1 (59%)	-0.408
	32353.8	0.078		-0.067
⁴D	32429.1	-0.004		0.003
	33593.8	-0.226		0.212
	33725.9	-0.033		-0.043
	34460.4	-0.256		0.226
	36053.0	0.777	0 1 1 1 2 (42%)	-0.021

Table S26: NEVPT2 transition energy and their individual contribution to the D values for Complex 19 (up to 17 quartets and 13 doublets are shown).

Complex 19	NEVPT2 Transition energies	D (cm ⁻¹)	Major CASSCF electronic Wave function $d_{xz}d_{yz}d_{x^2-y^2}d_{xy}d_{z^2}$	E (cm ⁻¹)
⁶S	0.000	0.000	1 1 1 1 1	0.000
⁴G	22065.0	0.640	1 2 1 0 1 (27%)	-0.014
	23171.0	-0.269	2 1 1 0 1 (29%)	0.237
	25056.3	-0.127		-0.163
	26583.2	-0.000		-0.004
	26781.1	-0.001		0.001
	27133.9	-0.000		0.000
	27760.4	-0.000		-0.000
	27811.6	-0.000		0.000
	27839.5	-0.000		0.000
⁴P	31173.3	-0.027		0.018
	31994.4	-0.423	2 1 0 1 1 (23%)	-0.369
	32264.9	0.056		-0.070
⁴D	32434.2	-0.006		0.006
	33527.6	-0.260		0.231
	33777.8	-0.017		-0.061
	34365.8	-0.241		0.214
	36056.6	0.755	0 1 2 1 1 (32%)	-0.026

Table S27: NEVPT2 transition energy and their individual contribution to the D values for Complex 20 (up to 17 quartets and 13 doublets are shown).

Complex 20	NEVPT2 Transition energies	D (cm ⁻¹)	Major CASSCF electronic Wave function $d_{yz}d_{xz}d_{x^2-y^2}d_{xy}d_z^2$	E (cm ⁻¹)
⁶S	0.000	0.000	1 1 1 1 1	0.000
⁴G	21525.4	0.667	2 1 1 1 0 (58%)	-0.019
	22160.4	-0.296	1 2 1 1 0 (57%)	0.314
	25229.0	-0.082		-0.092
	26195.1	-0.004		-0.000
	26423.1	-0.042		-0.052
	27264.1	-0.000		0.000
	27636.8	0.000		0.000
	27674.0	-0.000		0.000
	27784.1	-0.000		0.000
⁴P	30272.9	-0.062		0.034
	31317.7	-0.396	1 1 0 2 1 (38%)	-0.395
	31732.6	0.065		-0.132
⁴D	32485.5	0.000		-0.002
	33369.2	-0.071		0.073
	33628.0	-0.006		-0.055
	35438.8	-0.374		0.378
	36520.0	0.692	0 1 1 1 2 (34%)	-0.032

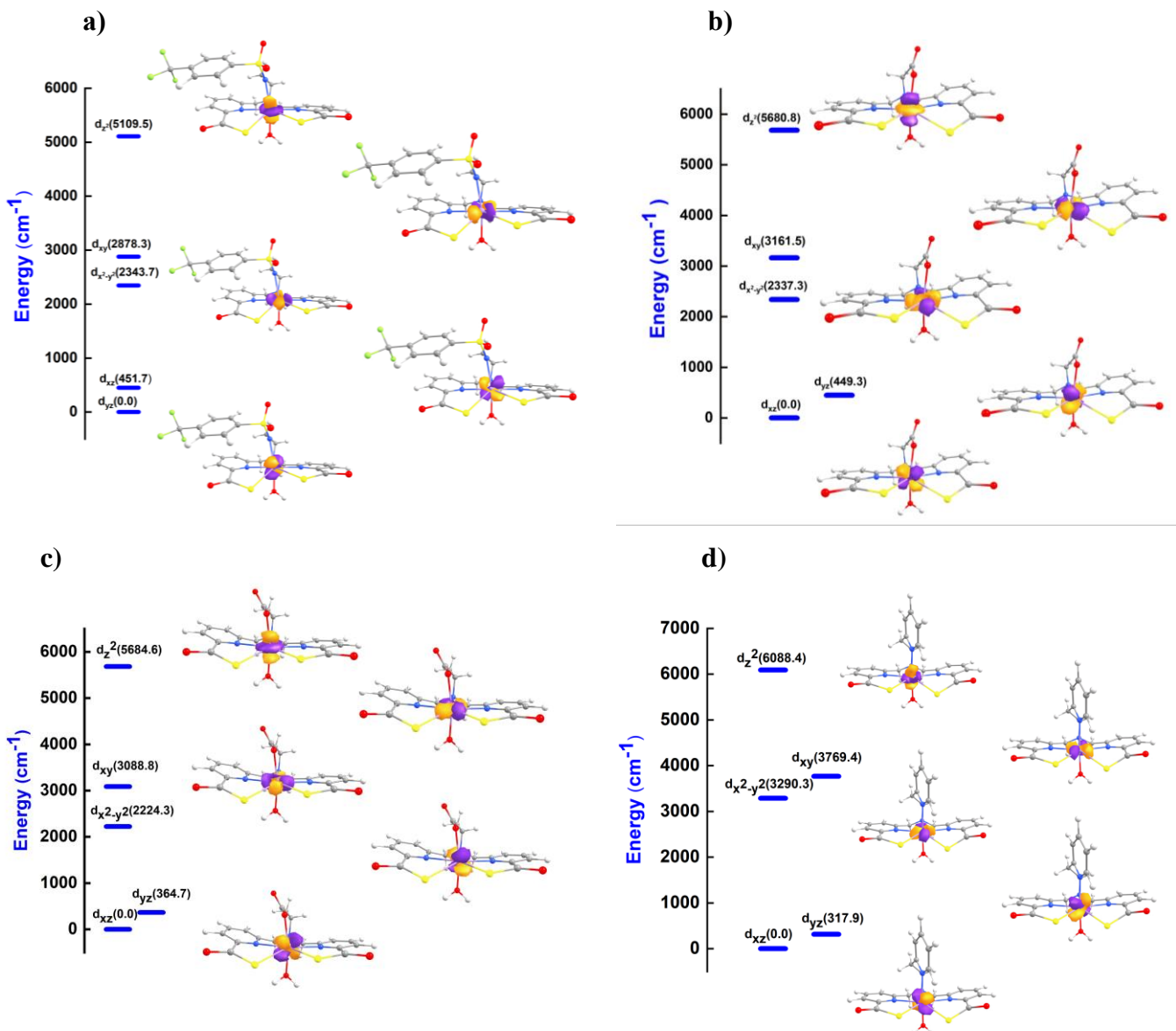


Figure S10: Splitting of metal d-orbitals obtained with AILFT calculations (a) Complex 5, (b) Complex 6, (c) Complex 7, and (d) Complex 8, respectively.

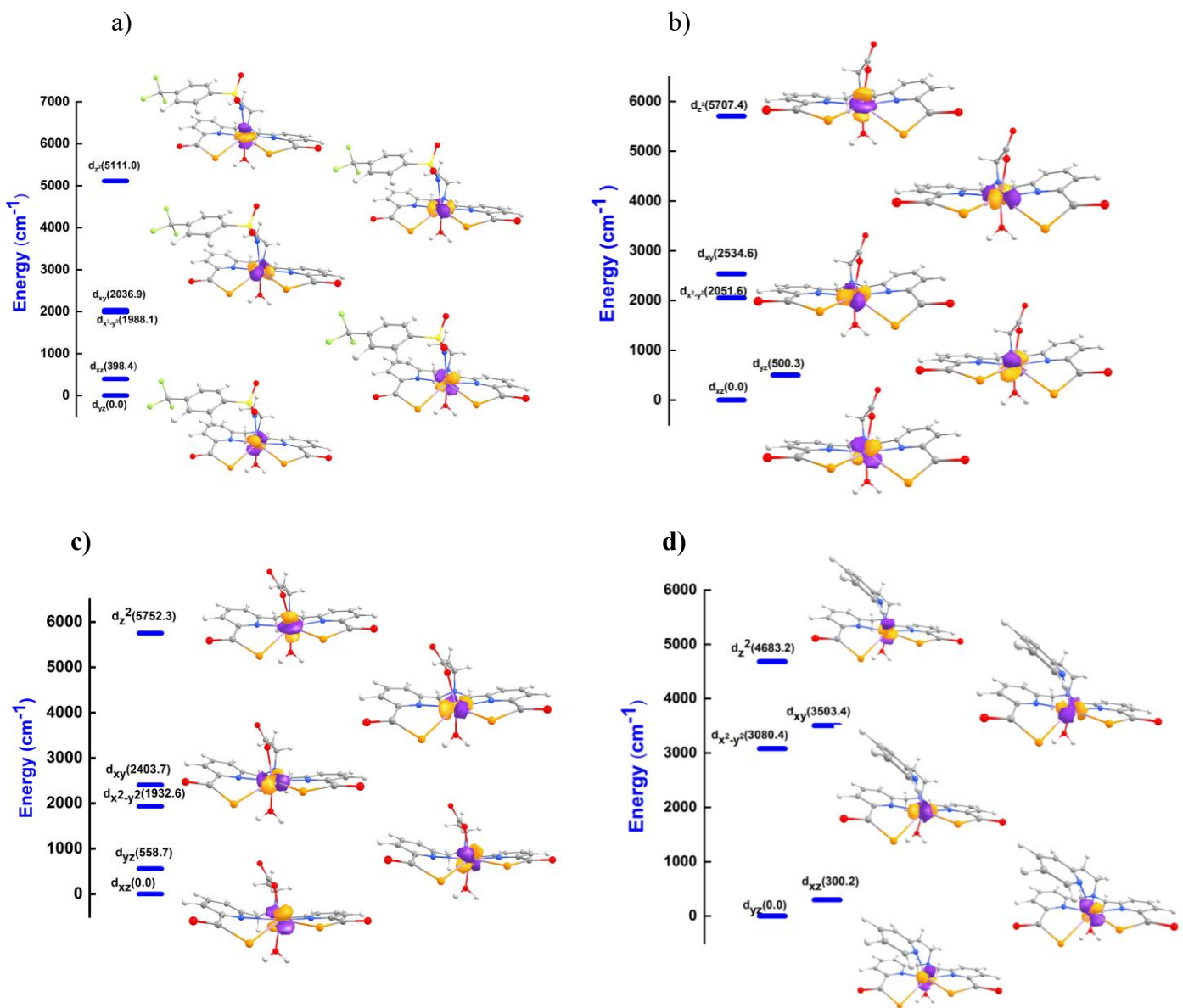


Figure S11: Splitting of metal d-orbitals obtained with AILFT calculations (a) Complex 9, (b) Complex 10, (c) Complex 11, and (d) Complex 12, respectively.

Table S28: Racah-parameters and spin-orbit coupling parameters for free Metal ion (Mn^{2+}) and complexes AILFT parameters (in cm^{-1}) from AILFT calculations.

Metal	Metal parameters	Complexes	Complex parameters
Mn^{2+}	$B^0=952.4$ $\zeta^0=319.6$	Complex 1	$B=900.3$ $\zeta=313.6$
		Complex 2	$B=903.9$ $\zeta=314.1$
		Complex 3	$B=904.0$ $\zeta=314.19$
		Complex 4	$B=903.7$ $\zeta=314.0$
Mn^{2+}	$B^0=952.4$ $\zeta^0=319.6$	Complex 5	$B=883.0$ $\zeta=312.14$
		Complex 6	$B=886.5$ $\zeta=312.26$
		Complex 7	$B=886.4$ $\zeta=312.27$
		Complex 8	$B=888.9$ $\zeta=312.39$
Mn^{2+}	$B^0=952.4$ $\zeta^0=319.6$	Complex 9	$B=882.1$ $\zeta=312.29$
		Complex 10	$B=886.4$ $\zeta=310.18$
		Complex 11	$B=883.4$ $\zeta=311.27$
		Complex 12	$B=886.1$ $\zeta=310.56$
		Complex 13	$B=900.7$ $\zeta=313.60$

Mn^{2+}	$B^0=952.4$ $\zeta^0=319.6$	Complex 14	$B=902.7$ $\zeta=314.07$
		Complex 15	$B=904.7$ $\zeta=316.1$
		Complex 16	$B=902.2$ $\zeta=313.78$
Mn^{2+}	$B^0=952.4$ $\zeta^0=319.6$	Complex 17	$B=899.3$ $\zeta=313.60$
		Complex 18	$B=903.5$ $\zeta=314.11$
		Complex 19	$B=902.3$ $\zeta=314.07$
		Complex 20	$B=904.1$ $\zeta=313.9$

Table S29: Topological parameters of the complexes analyzed here; the electron density at bond critical points (ρ_{bcp}), its Laplacian ($\nabla^2 \rho_{bcp}$), and the kinetic electron energy density (G_{bcp}). The results obtained at M06-2X/def2-TZVP level of approximation correspond to Mn-O, Mn-S, and Mn-Se bonds.

Complex	ρ_{bcp}	$\nabla^2 \rho_{bcp}$	G_{bcp}
Complex 1	Mn-O1=0.0508 Mn-O2=0.0467	Mn-O1=0.2415 Mn-O2=0.2174	Mn-O1=0.0664 Mn-O2=0.0595
Complex 2	Mn-O1=0.0509 Mn-O2=0.0497	Mn-O1=0.2431 Mn-O2=0.2352	Mn-O1=0.0668 Mn-O2=0.0646
Complex 3	Mn-O1=0.0495 Mn-O2=0.517	Mn-O1=0.2339 Mn-O2=0.2477	Mn-O1=0.0642 Mn-O2=0.0681
Complex 4	Mn-O2=0.0492 Mn-O3=0.0511	Mn-O2=0.2295 Mn-O3=0.2412	Mn-O2=0.0632 Mn-O3=0.0665
Complex 5	Mn-S1= 0.0374 Mn-S2=0.0324	Mn-S1= 0.1001 Mn-S2=0.0869	Mn-S1= 0.0306 Mn-S2=0.0257
Complex 6	Mn-S1=0.0340 Mn-S2=0.0392	Mn-S1=0.0911 Mn-S2=0.1059	Mn-S1=0.0272 Mn-S2=0.0326
Complex 7	Mn-S1=0.0339 Mn-S2=0.0389	Mn-S1=0.0908 Mn-S2=0.1053	Mn-S1=0.0271 Mn-S2=0.0323
Complex 8	Mn-S1=0.0330 Mn-S2=0.0376	Mn-S1=0.0869 Mn-S2=0.0995	Mn-S1=0.0260 Mn-S2=0.0305
Complex 9	Mn-Se1=0.0344 Mn-Se2=0.0276	Mn-Se1=0.0798 Mn-Se2=0.0639	Mn-Se1=0.0249 Mn-Se2=0.0190
Complex 10	Mn-Se1=0.0289 Mn-Se2=0.0364	Mn-Se1=0.0666 Mn-Se2=0.0853	Mn-Se1=0.0200 Mn-Se2=0.0269
Complex 11	Mn-Se1=0.0281	Mn-Se1=0.0649	Mn-Se1=0.0194

	Mn-Se2=0.0366	Mn-Se2=0.0857	Mn-Se2=0.0270
Complex 12	Mn-Se1=0.0365 Mn-Se2=0.0272	Mn-Se1=0.0833 Mn-Se2=0.0622	Mn-Se1=0.0265 Mn-Se2=0.0187

*(The numbering order of the atoms O1 and O2 are shown in Figure S8)

Table S30: NPA charge analysis obtained at the M06-2X/def2-TZVP level of theory.

Complexe 1		Complex 5		Complex 9	
Atom	Charge	Atom	Charge	Atom	Charge
Mn	1.036	Mn	0.601	Mn	0.566
O1	-0.744	S1	-0.243	Se1	-0.233
O2	-0.714	S2	-0.188	Se2	-0.170
Complex 2		Complex 6		Complex 10	
Atom	Charge	Atom	Charge	Atom	Charge
Mn	1.132	Mn	0.694	Mn	0.660
O1	-0.723	S1	-0.214	Se1	-0.660
O2	-0.733	S2	-0.275	Se2	-0.285
Complex 3		Complex 7		Complex 11	
Atom	charge	Atom	charge	Atom	Charge
Mn	1.146	Mn	0.696	Mn	0.662
O1	-0.727	S1	-0.272	Se1	-0.286
O2	-0.718	S2	-0.216	Se2	-0.187
Complex 4		Complex 8		Complex 12	
Atom	charge	Atom	Charge	Atom	charge
Mn	1.1016	Mn	0.551	Mn	0.499
O1	-0.732	S1	-0.205	Se1	-0.225
O2	-0.736	S2	-0.240	Se2	-0.169

Table S31: Mayer bond order obtained at the M06-2X/def2-TZVP level of theory.

Complex	Bond order	Complexes	Bond order	Complex	Bond order
Complex 1	Mn-O1=0.264 Mn-O2=0.296	Complex 5	Mn-S1=0.465 Mn-S2=0.384	Complex 9	Mn-Se1=0.452 Mn-Se2=0.397
Complex 2	Mn-O1=0.309 Mn-O2=0.289	Complex 6	Mn-S1=0.467 Mn-S2=0.401	Complex 10	Mn-Se1=0.465 Mn-Se2=0.387
Complex 3	Mn-O1=0.309 Mn-O2=0.281	Complex 7	Mn-S1=0.465 Mn-S2=0.400	Complex 11	Mn-Se1=0.456 Mn-Se2=0.378
Complex 4	Mn-O1=0.283 Mn-O2=0.278	Complex 8	Mn-S1=0.474 Mn-S2=0.438	Complex 12	Mn-Se1=0.492 Mn-Se2=0.356

Table S32: Atomic Cartesian coordinates (Å) of the PBE/GTH-DZVP optimized structure of the $[\text{Mn}(\text{dpasam})(\text{H}_2\text{O})]^-$ complex. Only the water molecules directly coordinated with the Mn^{2+} ion are included.

Atoms	X	Y	Z
Mn	2.07241700	6.14320700	3.49493600
C	-0.32453600	4.31113000	2.80211300
C	-0.85349300	5.11666600	3.98363300
C	-2.03134400	4.78678500	4.63012800
H	-2.60083600	3.93257700	4.29406900
C	-2.42972400	5.56702000	5.70734500
H	-3.33229100	5.32673200	6.25424600
C	-1.65907500	6.65746100	6.07450000
H	-1.94297300	7.29032100	6.90490700
C	-0.50051700	6.93351100	5.35431800
C	0.32552800	8.16812600	5.63385200
H	-0.12051400	8.97885500	5.05340500
H	0.22508200	8.44688000	6.68966600
C	2.28220100	9.28045200	4.72964300
H	2.47795500	10.00815300	5.52790400
H	1.55420300	9.72996400	4.05057400
C	3.54730400	9.03561700	3.94313700
C	4.55050800	9.99117500	3.83875900
H	4.46117200	10.92965800	4.36930000
C	5.65642000	9.71372200	3.05064200
H	6.45211800	10.44084800	2.95424400
C	5.73380100	8.49478400	2.39195500
H	6.57337900	8.22890700	1.76682400
C	4.69375900	7.59507100	2.55459300
C	4.67369300	6.23298600	1.86420900
C	2.55540600	7.51559900	6.34041200
H	2.38882900	8.10846600	7.24988700
H	3.60232800	7.62650400	6.05362700
C	2.29982500	6.04962400	6.63028400

H	2.90440800	5.76999500	7.49696900
H	1.24800100	5.90953400	6.91671000
C	1.24455200	2.99765200	5.97633600
C	0.64451700	2.27863200	4.95505100
H	1.16894400	2.13787800	4.01992800
C	-0.62586500	1.74851100	5.13939000
H	-1.10034500	1.19354100	4.34256100
C	-1.28199700	1.95478000	6.34117000
C	-0.68398800	2.67825000	7.36835400
H	-1.20517600	2.82658200	8.30566800
C	0.58709900	3.19405200	7.18954300
H	1.07744000	3.72621500	7.99372000
C	-2.67386100	1.43774200	6.55211400
N	-0.11004400	6.16266400	4.34742100
N	1.72599800	8.03236900	5.24277700
N	3.63479300	7.86769800	3.31535300
N	2.65359400	5.24805800	5.45893400
O	0.83174800	4.64294600	2.39709700
O	-1.04364200	3.42779100	2.33488200
O	3.64296000	5.53478500	2.08409500
O	5.63719200	5.93525500	1.15516600
O	3.56791600	3.46282100	6.97209800
O	3.39932100	3.08609300	4.54473900
O	1.07469700	7.35540000	1.71580200
H	1.73050900	7.65896900	1.07739000
H	0.71664500	6.53028900	1.35445000
S	2.86115400	3.72091600	5.72841600
F	-2.79690100	0.78324300	7.71642800
F	-3.57351800	2.43769100	6.58784800
F	-3.06694000	0.60097200	5.58762000

Table S33: Atomic Cartesian coordinates (Å) of the PBE/GTH-DZVP optimized structure of the [Mn(dpaaa)(H₂O)]⁻ complex. Only the water molecules directly coordinated with the Mn²⁺ ion are included.

Atoms	X	Y	Z
O	1.73738500	1.00839700	1.63782100
O	-1.18895700	1.33269000	1.60938400
O	3.91701700	1.28253100	2.05431600
N	2.22694900	-0.69887100	-0.31361300
N	-2.05282400	-0.50271100	-0.07659600
O	-3.26930000	1.79677300	2.28786700
C	-2.38605900	-1.50534500	-0.88264100
C	2.38719500	-1.58280100	-1.29344200
N	-0.00323500	-2.06433300	-1.08267600
C	2.96810900	0.78292400	1.44721900
C	3.28306700	-0.21930400	0.33821200
C	-4.28159200	-0.37396100	0.73264000
H	-4.98981700	0.10786300	1.39065800
C	3.64899300	-2.03539800	-1.65775000
H	3.75521000	-2.76577000	-2.44857600
C	-2.44316900	1.16530600	1.62532600
C	1.12840900	-2.01963800	-2.00352700
H	0.90940800	-1.27585200	-2.77317300
H	1.29772500	-2.97809200	-2.50945400
C	4.57618800	-0.60929600	0.02947900
H	5.40488900	-0.19479800	0.58447500
C	-2.96168200	0.05050900	0.71910300
C	-1.28306500	-2.00606700	-1.78195300
H	-1.56077600	-2.97425100	-2.21588100
H	-1.18691700	-1.29151000	-2.60263500
C	-3.68078600	-2.00593400	-0.91631600
H	-3.92677400	-2.83256000	-1.56916600
C	4.75562600	-1.53663400	-0.98690200

H	5.74923700	-1.87446400	-1.25113700
C	-4.63995900	-1.42507900	-0.09837600
H	-5.65650600	-1.79629100	-0.10498200
O	0.13218500	1.20616400	-1.38200700
H	0.91625600	1.73454000	-1.57234500
H	-0.62025300	1.80688000	-1.44240600
C	0.07187300	-3.20696800	-0.16842100
H	-0.49395000	-4.06122700	-0.55188400
H	1.11634100	-3.52119400	-0.08886700
C	-0.36222500	-2.93141300	1.28365500
Mn	0.15776700	-0.04965300	0.53911900
O	-0.86322300	-3.87122000	1.90589200
O	-0.10018200	-1.78358300	1.75777700

Table S34: Atomic Cartesian coordinates (Å) of the PBE/GTH-DZVP optimized structure of the [Mn(cbda)(H₂O)]⁻ complex. Only the water molecules directly coordinated with the Mn²⁺ ion are included.

Atoms	X	Y	Z
Mn	0.13702300	-0.91095400	-0.08046600
N	-2.03102400	-0.17051000	-0.59158900
C	-2.98565800	-1.02256000	-0.23398400
C	-4.31149800	-0.63243800	-0.11753700
H	-5.05666700	-1.35932700	0.17056800
C	-4.62958700	0.69451300	-0.36554900
H	-5.65089700	1.03994700	-0.27178300
C	-3.62356100	1.58102100	-0.72442400
H	-3.83661800	2.62457700	-0.91443500
C	-2.32449000	1.10373900	-0.83288500
C	-1.16160500	1.95768900	-1.27046400
H	-0.93425800	1.68869300	-2.30475200
H	-1.44502300	3.01451500	-1.27155900
N	0.03135300	1.67812900	-0.47457100

C	1.25136200	2.10884400	-1.14892000
H	1.43700700	3.18497900	-1.04767000
H	1.14267500	1.90635600	-2.21741700
C	2.45520400	1.33913000	-0.65776400
C	3.72734800	1.89699700	-0.62217200
H	3.87340700	2.93020800	-0.90746800
C	4.79128600	1.10778200	-0.21345000
H	5.79155300	1.51925300	-0.17723900
C	4.55881700	-0.20883700	0.15715500
H	5.35142700	-0.86309500	0.48875500
C	3.25872200	-0.68399900	0.10561000
N	2.24304500	0.07718900	-0.29692600
C	-2.51730100	-2.44687900	0.05982300
O	-1.26349000	-2.61266000	0.06191800
O	-3.38097200	-3.30156400	0.27097000
C	-0.03181500	2.18942800	0.91516000
H	1.00519600	2.19517000	1.26493000
C	-0.72189200	1.18130100	1.87217100
O	-0.30428500	-0.01857200	1.80234400
C	-0.59177600	3.59795100	1.04713300
H	-0.12006000	4.27712900	0.33454600
H	-0.40210700	3.97145500	2.05129900
H	-1.67044900	3.61446200	0.89158400
C	2.89295000	-2.10948900	0.51513000
O	1.65833000	-2.38374200	0.47620700
O	3.81017700	-2.86331400	0.84563000
O	0.34963200	-1.17147900	-2.33711300
H	1.12369900	-0.89015800	-2.83690000
H	-0.41198900	-1.08490300	-2.92102000
O	-1.56253400	1.59955200	2.66899500

Table S35: Atomic Cartesian coordinates (\AA) of the PBE/GTH-DZVP optimized structure of the [Mn(pydpa)(H₂O)] complex. Only the water molecules directly coordinated with the Mn²⁺ ion are included.

Atoms	X	Y	Z
Mn	7.39500000	9.37600000	8.17700000
O	6.07600000	11.00600000	7.32200000
O	7.41000000	10.99900000	9.79000000
N	7.05100000	8.94300000	5.98800000
N	8.60100000	8.59200000	9.81100000
O	5.12200000	11.86900000	5.49700000
O	7.40700000	11.02000000	12.03700000
N	5.51700000	8.35300000	9.17800000
N	8.14800000	7.02900000	7.59500000
C	8.59100000	9.30200000	10.94300000
C	6.37100000	9.86200000	5.28700000
C	5.78900000	10.98500000	6.08600000
C	7.67300000	7.96000000	5.34800000
C	7.73800000	10.52900000	10.92300000
C	5.46900000	7.10700000	9.68100000
C	9.35500000	7.50200000	9.70900000
C	4.51500000	9.20500000	9.46800000
H	4.59900000	10.19200000	9.03000000
C	7.66300000	7.87400000	3.96200000
H	8.18300000	7.05500000	3.47700000
C	6.29200000	9.82300000	3.91000000
H	5.74200000	10.59200000	3.38600000
C	4.43100000	6.71800000	10.52200000
H	4.42000000	5.70900000	10.91400000
C	9.34600000	8.93700000	12.03800000
H	9.30800000	9.53700000	12.93400000
C	3.44100000	8.86300000	10.26000000
H	2.65500000	9.58300000	10.45000000
C	10.16800000	7.10200000	10.75900000

H	10.79400000	6.22900000	10.64700000
C	8.45100000	6.97500000	6.16600000
H	8.29700000	5.96900000	5.75500000
H	9.51100000	7.19100000	6.01600000
C	6.96600000	8.81700000	3.23800000
H	6.94300000	8.77700000	2.15800000
C	3.41100000	7.59500000	10.81700000
H	2.59400000	7.28800000	11.45500000
C	7.02800000	6.11100000	7.88000000
H	7.34300000	5.08900000	7.63400000
H	6.21700000	6.35800000	7.19100000
C	10.15600000	7.82000000	11.93600000
H	10.77500000	7.51200000	12.76900000
C	6.51400000	6.10000000	9.31200000
H	7.34600000	6.15200000	10.02000000
H	6.08200000	5.11200000	9.48800000
C	9.32200000	6.74300000	8.41700000
H	10.21700000	7.02300000	7.85700000
H	9.41500000	5.67800000	8.64000000
H	9.88900000	10.59200000	8.21900000
H	9.50600000	10.55900000	6.68600000
O	9.58500000	9.97400000	7.50500000